Journal Pre-proofs

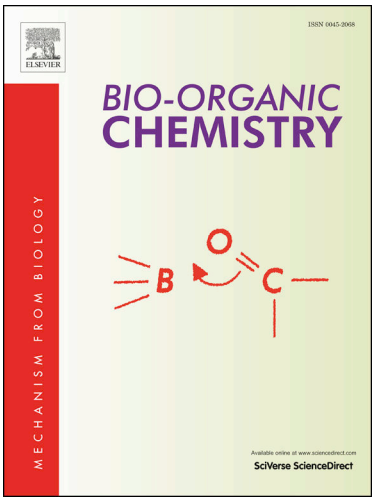

Drug-Like Property Optimization: Discovery of Orally Bioavailable Quinazoline-Based Multi-Targeted Kinase Inhibitors

Shu-Yu Lin, Chun-Feng Chang, Mohane Selvaraj Coumar, Pei-Yi Chen, Fu-Ming Kuo, Chun-Hwa Chen, Mu-Chun Li, Wen-Hsing Lin, Po-Chu Kuo, Sing-Yi Wang, An-Siou Li, Chin-Yu Lin, Chen-Ming Yang, Teng-Kuang Yeh, Jen-Shin Song, John T.A. Hsu, Hsing-Pang Hsieh

PII: S0045-2068(20)30031-6
DOI: https://doi.org/10.1016/j.bioorg.2020.103689
Reference: YBIOO 103689

To appear in: *Bioorganic Chemistry*

Received Date: 6 January 2020
Revised Date: 19 February 2020
Accepted Date: 20 February 2020

Please cite this article as: S-Y. Lin, C-F. Chang, M. Selvaraj Coumar, P-Y. Chen, F-M. Kuo, C-H. Chen, M-C. Li, W-H. Lin, P-C. Kuo, S-Y. Wang, A-S. Li, C-Y. Lin, C-M. Yang, T-K. Yeh, J-S. Song, J.T.A. Hsu, H-P. Hsieh, Drug-Like Property Optimization: Discovery of Orally Bioavailable Quinazoline-Based Multi-Targeted Kinase Inhibitors, *Bioorganic Chemistry* (2020), doi: https://doi.org/10.1016/j.bioorg.2020.103689

Drug-Like Property Optimization: Discovery of Orally Bioavailable Quinazoline-Based Multi-Targeted Kinase Inhibitors

Shu-Yu Lin[a,#], Chun-Feng Chang[a,#], Mohane Selvaraj Coumar[d,#], Pei-Yi Chen[a], Fu-Ming Kuo[a], Chun-Hwa Chen[a], Mu-Chun Li[a], Wen-Hsing Lin[a], Po-Chu Kuo[a], Sing-Yi Wang[a], An-Siou Li [a], Chin-Yu Lin[a], Chen-Ming Yang[a], Teng-Kuang Yeh[a], Jen-Shin Song[a], John T.-A. Hsu[a], Hsing-Pang Hsieh [a,b,c*]

[a]Institute of Biotechnology and Pharmaceutical Research, National Health Research Institutes, 35 Keyan Road, Zhunan, Miaoli County 35053, Taiwan, R.O.C.
[b]Department of Chemistry, National Tsing Hua University, Hsinchu, 30013, Taiwan
[c]Frontier Research Center on Fundamental and Applied Sciences of Matters, National Tsing Hua University, Hsinchu, 30013, Taiwan
[d]Centre for Bioinformatics, School of Life Sciences, Pondicherry University, Kalapet, Puducherry 605014, India.

[#]These authors contributed equally to this work.

*To whom correspondence should be addressed: Prof. Dr. Hsing-Pang Hsieh, Phone, +886-37-246-166 ext. 35708; fax, +886-37-586-456; e-mail, hphsieh@nhri.org.tw

Abstract

In an effort to develop new cancer therapeutics, we have reported clinical candidate BPR1K871 (**1**) as a potent anticancer compound in MOLM-13 and MV4-11 leukemia models, as well as in colorectal and pancreatic animal models. As BPR1K871 lacks oral bioavailability, we continued searching for orally bioavailable analogs through drug-like property optimization. We optimized both the physicochemical properties (PCP) as well as *in vitro* rat liver microsomal stability of **1**, with concomitant monitoring of aurora kinase enzyme inhibition as well as cellular anti-proliferative activity in HCT-116 cell line. Structural modification at the 6- and 7-position of quinazoline core of **1** led to the identification of **34** as an orally bioavailable (F% = 54) multi-kinase inhibitor, which exhibits potent anti-proliferative activity against various cancer cell lines. Quinazoline **34** is selected as a promising oral lead candidate for further preclinical evaluation.

Keywords: aurora kinase inhibitor, quinazoline, physicochemical property, metabolic stability, oral bioavailability, anti-cancer

1. Introduction

Cancer is a global disease with high mortality rate. Lung, breast, prostate and colorectal cancer are the major cancer types reported world over [1]. Many pharmaceutical companies and academic institutes are in pursuit of novel anti-cancer therapeutics that could target aberrant proteins/pathways responsible for the development or progression of cancer [2]. One of the important classes of drug targets for anti-cancer drug development are protein kinases [3-5]. Protein kinases are enzymes that transfer phosphate group from ATP to serine, threonine or tyrosine residues in proteins; phosphorylation of proteins acts as a switch to turn-on or turn-off the proteins function, thereby playing an important role in normal physiological signaling process. More than 500 protein kinases have been identified in the humans that are involved in a variety of function and maintain homeostasis [5]. Aberration in many protein kinase signaling process has been reported, either due to the overexpression or due to mutations in the protein. These signaling aberrations results in alteration in normal cellular functions, leading to a variety of diseases, including cancer [6, 7].

During the last two decades, researches have shown that the altered kinase responsible for the cancer could be targeted by ATP competitive small molecule inhibitors. These small molecules bind to the ATP binding site of the protein kinase and block the aberrant downstream signaling, resulting in the inhibition of cancer progression [3, 6,

8]. For example, in 2001 the first kinase inhibitor imatinib (Gleevec®) was approved by U.S. Food and Drug Administration (FDA) for the treatment of chronic myeloid leukemia (CML). Imatinib targets the ATP site of Abl kinase and prevents the progression of the disease caused by the Bcr-Abl fusion protein [9, 10]. Currently, 52 small molecule inhibitors that target various kinase (Abl, EGFR, HER2, etc) have been approved world over for the treatment of various cancers (CML, lung cancer, breast cancer, etc) [5, 7, 8, 11]. The successful launch of several kinase inhibitors endorses the strategy of blocking the aberrant kinase as a new avenue for targeted cancer therapy. Aurora kinase belongs to serine/threonine kinase family and are normally expressed during mitosis process. There are three distinct subtypes – Aurora A kinase , Aurora B kinase and Aurora C kinase – with different function and location in the nucleus, regulating the mitosis process [12]. Aurora A is located to the central of the chromosome and to the pole of spindle which is involved in the process of centrosome maturation and separation. Aurora B is a component of the chromosomal passenger complex (CPC) that plays a critical role in the mitosis process; Aurora B is essential for chromosomal condensation and cytokinesis. The third subtype Aurora C kinase has high similarity and overlapped functions with Aurora B. Aurora A/B have been found to be overexpressed or amplified in many malignant tumors, like glioma, breast, lung, ovarian, colon and thyroid cancers. To date, several Aurora kinase inhibitors have been

reported to show anti-cancer efficacy in pre-clinical animal models and few are in different stage of clinical trial as anti-cancer therapeutics [13–17] (**Figure 1**). These observations led us to develop different series of inhibitors against Aurora kinase for the treatment of cancers [18–20].

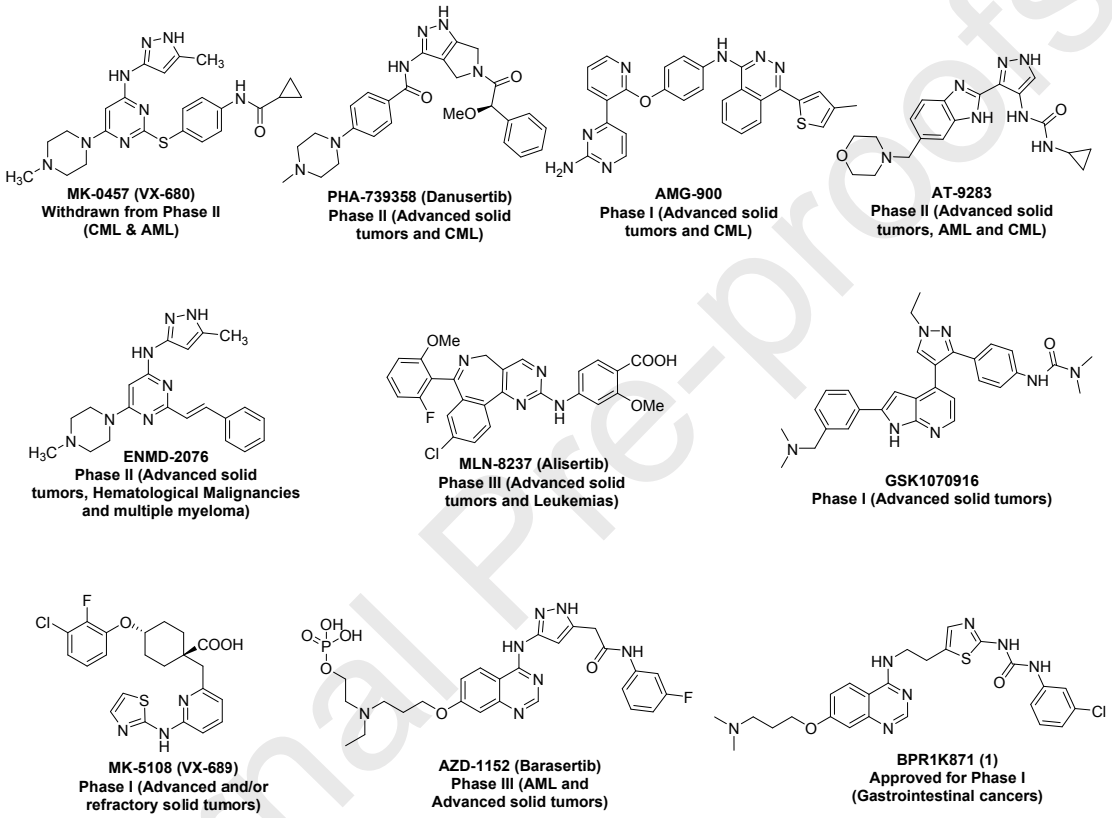

Figure 1. Representative Aurora kinase inhibitors in clinical trials. BPR1K871 (**1**) is a quinazoline based multi-kinase inhibitor with Aurora and FLT3 kinase inhibition reported by us.

In our previous effort to develop Aurora kinase inhibitors, compound **2** was identified as initial hit from a kinase-focused furanopyrimidine library as Aurora kinase A inhibitor (**Figure 2**). The following introduction of a phenylurea group on the aniline

of **2** gave compound **3** as a potent hit, with 14.8-fold enhanced Aurora kinase inhibition [21]. In continuation works, we reported utilizing 3D-QSAR-assisted drug design and a FLT3 homology model to develop two potential lead compounds, **4** with quinazoline core and **5** with a thiazole containing urea chain [22, 23].

As the quinazoline core is considered as a privileged structure for the inhibition of ATP-dependent kinases with lower lipophilicity, a series of lead-to-candidate optimization led to the identification of BPR1K871 (**1**) as a multi-kinase inhibitor with potent enzymatic (Aurora A IC_{50} = 22 nM; Aurora B IC_{50}= 13 nM; FLT3 IC_{50} = 19 nM) and cellular activities in AML and multiple solid tumor cell lines. In addition, the inhibitor **1** demonstrated *in vivo* efficacy in leukemia (MOLM-13 and MV4-11), colorectal (COLO205) and pancreatic (Mia-PaCa2) xenograft mouse models upon intravenous (IV) administration [18]. Currently, **1** has been approved as investigational new drug (IND) by US FDA and TDFA for testing in humans for gastrointestinal cancers or gastroenterology and hepatology related cancer treatment.

Notably, the majority of the medical indication of kinase inhibitors are approved for the treatment of malignancies as oral oncologics, since oral prescription drugs offer a number of advantages including easy storage, lower costs, patient preference and convenience, etc. However the IND candidate **1** could not be developed as oral drug due to poor oral bioavailability and need to be administered though IV route in clinics.

Due to this drawback, we undertook the optimization of **1** for the identification of orally bioavailable compounds with anticancer potential in this work For this purpose, the substitutions at three different possible metabolic sites in **1**, the C-6 and C-7 position of the quinazoline core and CH_2CH_2 linker of thiazole urea side chain, were modified to alter the drug-like properties while maintaining the Aurora kinase enzymatic as well as cellular anticancer activities.

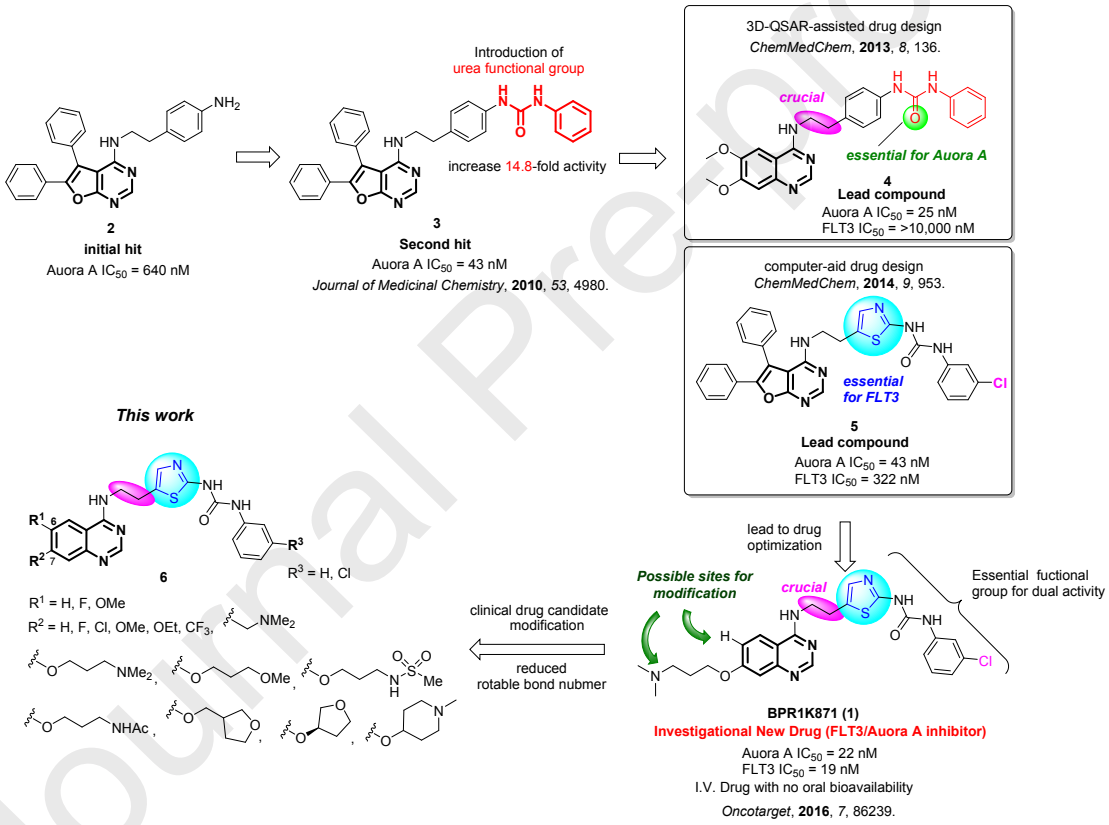

Figure 2. Flow chart illustrating the discovery of drug candidate BPR1K871 (**1**) and the design strategy in this work for improving oral bioavailability of **1**.

2. Chemistry

One of the key intermediate **7** was prepared according to our previous reports [18].

The chloro group of **7** was replaced by nucleophilic substitution with sodium methoxide to give **8**. On the other hand, substitution with sodium azide, followed by hydrogenation over Pd/C provided the amine **10**. Reacting **10** with methanesulfonyl chloride or acetic anhydride produced the corresponding sulfonamide **11** and the acetamide **12**.

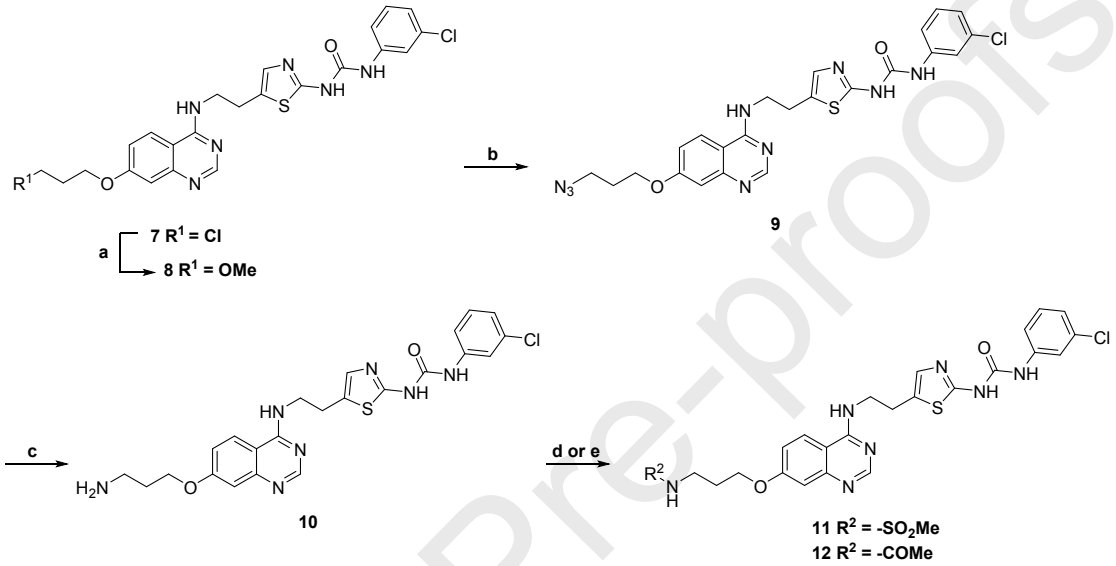

Scheme 1. Reaction conditions and reagents: (a) NaOMe, KI, DMF, 100 °C, 16 h, 34%; (b) NaN_3, DMSO, 60 °C, 16 h, 95%; (c) H_2, 10% Pd/C, rt, 16 h, 64%; (d) $MeSO_2Cl$, Et_3N, DMF, CH_2Cl_2, rt, 16 h, 15%; (e) Ac_2O, pyridine, CH_2Cl_2, rt, 48 h, 35%.

For compounds **16**–**37**, quinazolinone derivatives **13a**–**v** were either commercially available or prepared according to reported methods. The starting quinazolinone **13a**–**v** were first chlorinated by thionyl chloride or phosphoryl chloride, followed by nucleophilic aromatic substitution with *tert*-butyl 5-(2-aminoethyl)thiazol-2-yl-carbamate to give **14a**–**v**. De-protection of the Boc group of **14a**–**v** under acidic

condition gave the key intermediates **15a–v**. Reaction of phenyl isocyanate or 3-chlorophenyl isocyanate with **15a–v** gave the final urea compounds **16–37**.

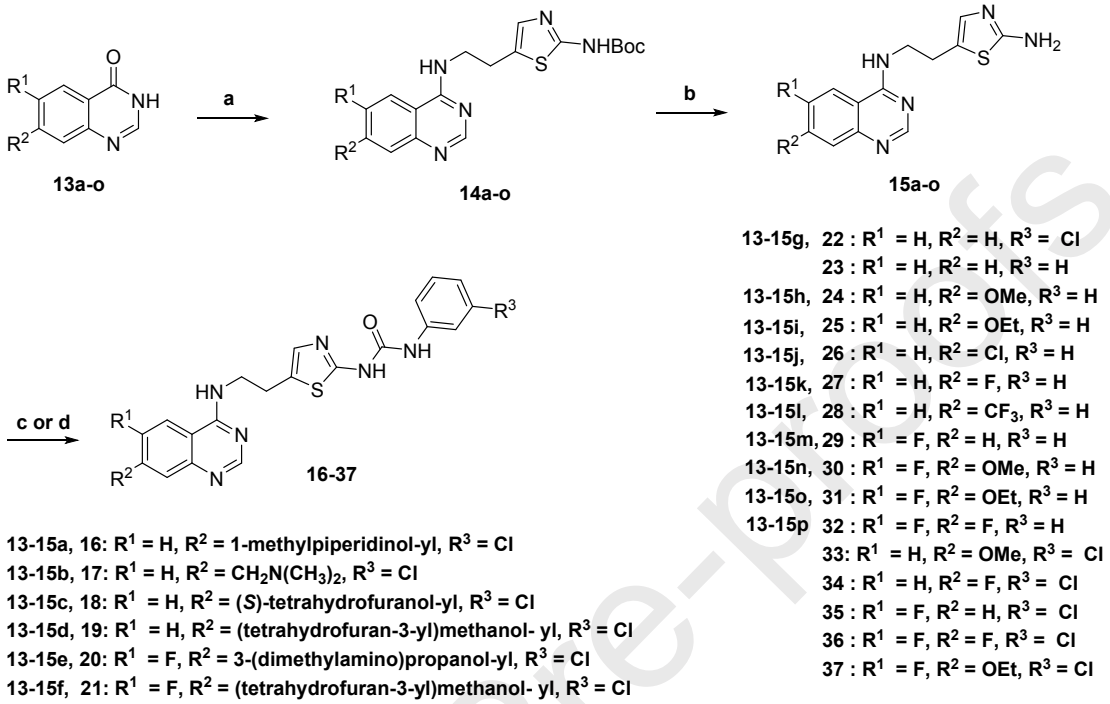

Scheme 2. Reaction conditions and reagents: (a) (i) $SOCl_2$ or $POCl_3$, DMF, reflux, 15 h, (ii) *tert*-butyl 5-(2-aminoethyl)-thiazol-2-yl carbamate, Et_3N, EtOH, reflux, 15 h, 28–97% for two steps; (b) 6.0 N $HCl_{(aq)}$, rt, 10 h, 58–99% or TFA, CH_2Cl_2, rt, 12 h, 62%; (c) 3-Cl-PhNCO, MeOH, CH_2Cl_2, rt, 16 h, 21-86%; (d) PhNCO, MeOH, CH_2Cl_2, rt, 16 h, 19–94%.

In a manner similar to compounds **16–37**, compound **40** was prepared by nucleophilic aromatic substitution of the 4-chloro quinazoline **38** [24] with *tert*-butyl 5-(2-aminoethyl)thiazol-2-yl-carbamate. De-protection of **39** under acidic condition, followed by reaction with 3-chlorophenyl isocyanate installed the urea group in **40**.

Nucleophilic substitution reaction of compound **40** with dimethylamine gave the desired compound **41**.

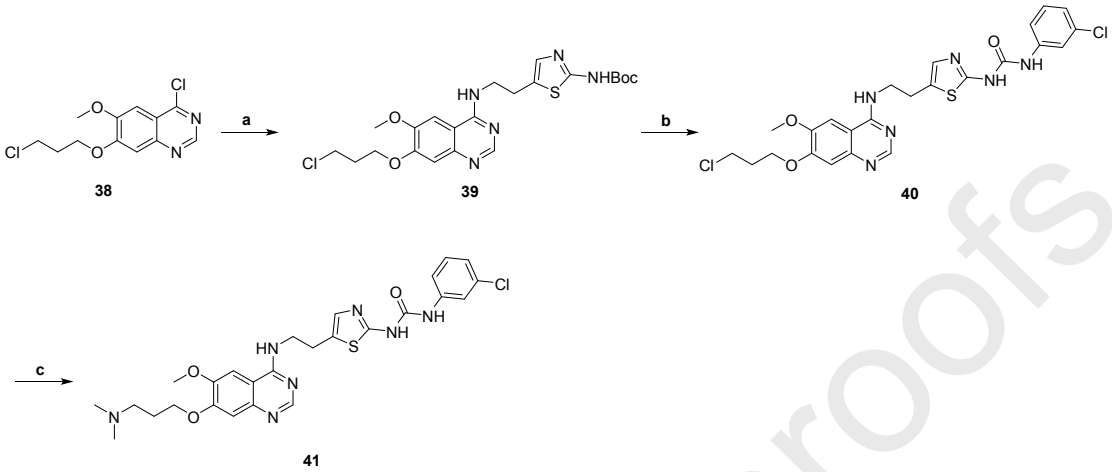

Scheme 3. Reaction conditions and reagents: (a) *tert*-butyl 5-(2-aminoethyl)-thiazol-2-ylcarbamate, Et_3N, EtOH, reflux, 16 h, 78%; (b) (i) TFA, CH_2Cl_2, rt, 2 h, (ii) 3-Cl-PhNCO, MeOH, CH_2Cl_2, rt, 16 h, 66% for two steps; (c) 40% $(CH_3)_2NH_{(aq)}$, DMF, reflux, 3 h, 80%.

3. Results and discussion

Biological evaluation of Aurora A /B kinase inhibitory activities and SAR analysis

All the synthesized key compounds were evaluated for their Aurora A/B inhibitory activities using the previously established Aurora kinase assay and cellular activity in HCT-116 colon cancer cell line, as well as acute cellular toxicity in Detroit 551 embryonic skin cell lines [18,19]. The compounds were also evaluated for their metabolic stability in *in vitro* rat liver microsomal stability (RLMS) assay, to select the compound with favorable PK properties and good stability for further *in vivo* PK study

[25]. The microsomal stability assay is used to primarily investigate *in vitro* intrinsic clearance of a compound under phase I metabolism and offer an approach for prediction of the hepatic metabolism of an inhibitor in drug candidate development pipeline. The 50% inhibitory concentrations for Aurora kinase enzymatic assays (IC_{50}) and cell growth (CC_{50}), the selectivity indices (SI; CC_{50} of Detroit 551/HCT-116) as well as rat liver microsomal stability are presented in Tables 1 and 2. Compound **1** was used as the starting point for the structure-activity and drug optimization studies.

In the field of medicinal chemistry, Lipinski's rule of five and Veber's rule are the guideline for medicinal chemist searching drug-like chemical properties with oral effective potential. It is understood that fine tuning the physicochemical properties (PCPs) of a lead molecule could alter the ADME property [26-30]. Hence, close scrutiny was placed on the PCPs, by calculating the guiding parameters including molecular weight (MW), number of hydrogen bond acceptors (HBA), number of hydrogen bond donors (HBD), calculated LogP (cLogP), number of rotatable bonds (NRB) and polar surface area (PSA) [30-32]. Compounds with optimal PCPs (MW < 500, HBA <10, HBD <5, LogP < 5, NRB < 10 and PSA < 140 $Å^2$) have higher probability for oral absorption. The clinical candidate **1** showed no oral bioavailability and had high clearance *in vivo*. Only 14.5% of the drug remained after 30 minutes incubation with rat liver microsomes, suggesting faster drug metabolism could be one

reason for poor oral bioavailability. In addition, it was found to violate two of the empirical PCP guidelines (MW>500; NRB>10).

The initial focus of optimization was on the side chain bearing the solubilizing group attached to the 7-position of quinazoline core of **1**. In our previous studies with different heteroaromatic core structures for kinase inhibition, we have shown that introduction of *N,N*-dimethylamino solubilizing group into the heteroaromatic core structures resulted in improved kinase inhibition as well as anti-proliferative activity [18, 19]. However, it may be noted that oxidative deamination or *N*-demethylation of substituted amine is one of the most common phase I metabolic reaction carried out by cytochrome 450 (CYP) [33]. The metabolic reaction could inactivate a drug and also lower oral bioavailability. Hence, we replaced the terminal *N*,*N*-dimethyl group in the solubilizing side chain with alternate groups including methoxide, methylsulfonamide and acetamide (i.e., **8** ,**11**, **12**). The replacements enhanced the Aurora kinase inhibition potency, microsomal stability and selectivity as well as cellular activity in HCT-116 cell assay, as compared to the lead **1**.

The ability to alter the metabolic stability along with the retention of biological activity, further enthused us to modify the solubilizing side chain. To add rigidity and decrease the flexibility of the solubilizing side chain at 7-position of quinazoline core, compounds **16**–**19** were synthesized. The rigid cyclic functional group with less NRB

at 7-position maintained their bioactivity against Aurora A and improved microsomal stability, but increased the toxicity in Detroit 551 cell line (cf. **16**, **18**, and **19** with CC_{50} = 1.3–1.8 μM). The tetrahydrofuran-3-yl-methoxy group displayed 8.1-fold more cellular activity in HCT-116 assay than **1** (cf. **1** *versus* **19**). Modification of the solubilizing dimethylaminopropoxy moiety of **1** by replacement with dimethylaminomethyl group resulted in loss of potency for both Aurora A/B inhibition (cf. **1** *versus* **17**).

In addition, we have introduced an electron-donating methoxy group and electron-withdrawing fluoro groups onto the C-6 position of the lead **1** to give compounds **41** and **20**, respectively. Both compounds **20** and **41** showed improved stability (4.4–5.4-fold) in rat liver microsome, as compared to **1**. Even though the two compounds showed good aurora kinase inhibition, the methoxy bearing **41** showed poor growth inhibition against HCT-116 cells. Introduction of F-substituent at C-6 position of **1** enhanced 10.5-fold of the anti-proliferarive activity in HCT-116 assay with a selectivity indices of 403. Encouraged by the activity of 6-fluoro substituted analog **20**, a F-substituent was also introduced at the C-6 position of **19** to obtain compound **21**, which has similar level of metabolic stability and anti-proliferative activity in HCT-116 with a selectivity ratio of 115. Replacement of *N,N*-dimethylamino solubilizing functional group at 7-position led to increased microsomal stability while retaining its bioactivities,

suggesting the substitution of the 7-position *N,N*-dimethylamino moiety is tolerated.

Moving forward to reduce the molecular weight and the number of rotatable bonds in the inhibitors, for complying with PCPs guidlines, we investigated compound **22** with removal of substituent group from 7-postion of the quinazoline core and compound **23** with additionally lacking the 3-Cl substitution in the terminal phenyl ring of the urea side chain of **1** (**Table 2**). Both **22** and **23** displayed excellent Aurora enzymatic inhibition and cellular growth inhibitory activity as well as higher microsomal stability than that of **1** (cf. **1** *versus* **22** and **23**). Encouraged by these results that the removal of functional groups were well tolerated at quinazoline ring, compounds **24**–**34** were synthesized by attaching electron-donating (ethoxy and methoxy) and electron-withdrawing (chloro, fluoro and trifluoromethyl) groups at the C-6 and C-7 position of the quinazoline ring. All these compounds showed improved metabolic stability (RLMS = 41–80%) compared with the inhibitor **1**. Moreover, most of these compounds retained the Aurora A inhibition and had improved anti-proliferative activity in HCT-116 cell line, except for compound **28** with trifluoromethyl group. Particularly, compound **34** with a 7-F substitutent, had enhanced Aurora kinase activity (IC_{50}, Aurora A IC_{50}= 9 nM, Aurora B IC_{50}= 30.5 nM) and anti-proliferative activity in HCT-116 assay with high selectivity (i.e. **34**, CC_{50} = 16.0 nM; SI > 900-fold). Moreover, all of the target compounds reported in Table 2 possessed

good PCPs within the acceptable cut-off limits for oral bioavailability/drug-likeness. Based on the *in vitro* potency, microsomal stability, toxicity and PCPs profile, we selected compounds **20**–**23**, **27**, and **34** to perform *in vivo* PK studies.

***In vivo* pharmacokinetics investigation of selected compounds**

Before we embarked to investigate the *in vivo* pharmacokinetics profile of promising compounds, we carried out ADMET prediction using the Discovery Studio software. The ADMET descriptor model predicts human intestinal absorption (HIA) and blood-brain penetration (blood brain barrier, BBB) after oral administration. This model was developed using the method reported by Egan et al. [34, 35], which ulilize multivariate pattern recognition based on the predicted PSA and AlogP property (atom-type partition coefficient) with 95% and 99% confidence as ellipses. Well-absorbed compounds are expected to be found within the 95% confidence ellipse region. And in general, oral absorption tends to drop off quite rapidly outside the 95% ellipse region. Compound **1** with no oral bioavailability in rat PK study was located outside 95% ellipse, and compounds **11** and **12** were found outside the 99% ellipse duo to high PSA (> 140 $Å^2$).

According to the prediction model, **22**, **23**, **27**, and **34** with no violated PCPs are considered likely to be well-absorbed.

Based on the PCPs profile, RLMS, *in vitro* Aurora kinase inhibition and selective

anti-proliferative activity in HCT-116, **20**–**23**, **27**, and **34** were selected to carry out *in vivo* pharmacokinetic studies in rats (**Table 4**). We found that both **20** and **21** showed poor oral bioavailability (**20**, F = Not detected; **21**, F = 6 %) similar to **1**, despite **20** and **21** possessed higher *in vitro* metabolic stability. Notably, compound **22** showed 30% and **23** showed 46% oral bioavailability by removal of the substituent from quinazoline core. These encouraging results suggest that compounds with good *in vitro* metabolic stability and appropriate PCPs would have acceptable oral bioavailability. Next, **27** and **34** with a 7-fluoro group in the quinazoline ring were chosen for PK evaluation, as they possessed a high RLM stability and optimal *in vitro* activity profile. Accordingly, **34** was found to have better drug exposure on IV administration with 5-fold improved AUC and only 1/4th the clearance as that of the initial clinical candidate BPR1K871 (**1**). Moreover, oral administration of **34** resulted in an oral bioavailability of 54% and high AUC, making it feasible for oral administration during pharamodynamics evaluation in *in vivo*. The results indicated that compounds **22**, **23**, **27**, and **34** with acceptable oral absorption were located inside innermost oval in the ADMET prediction model.

Table 1. SAR investigations of compound **1,** focusing on the quinazoline ring substitutions.[a.b]

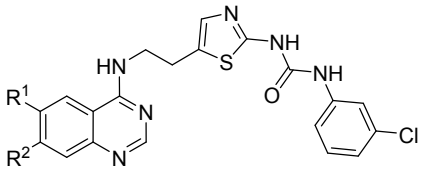

compound no.	R^1	R^2	RLMS (%)	Aurora A IC_{50} (nM)	Aurora B@ 100 nM	HCT-116 CC_{50} (nM)	Detroit 551 CC_{50} (μM)	Selectivity (Detroit 551/HCT-116 CC_{50})
1 (BPR1K871)	H	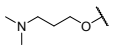	14.5	22	IC_{50} = 13 nM	141	4.0	29
8	H	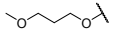	39.1	14.0	74%	22.4	1.8	80
11	H	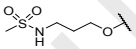	61.5	4.0	80%	67.0	2.7	40
12	H	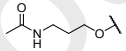	59.9	8.0	82%	46.4	5.8	125

16	H	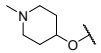	81.6	38.0	ND	320.4	1.4	4
17	H		41.3	262.0	7%	2962	N.D.	N.D
18	H		74.5	26.0	55%	119.7	1.3	11
19	H	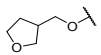	52.3	22.0	83%	17.4	1.8	103
41	OMe	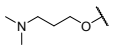	75.7	6.0	IC_{50} = 12 nM	287.7	12.6	44
20	F	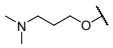	63.8	10.0	86%	13.4	5.4	403
21	F	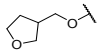	66.3	15.9	78%	44.4	5.1	115

[a]The rat liver microsomal stability (RLMS) assays offer a method to evaluate the rate of hepatic metabolism of a compound in liver microsomal incubation. Data was represented as % remaining at 30 min by incubation of the compound in rat microsomes.; [b]IC_{50} values represent the mean of at least two independent experiments.; N.D.: Not determined.

Table 2. SAR investigations of compound **1**, focusing on both the quinazoline ring and urea side chain substitutions.[a,b]

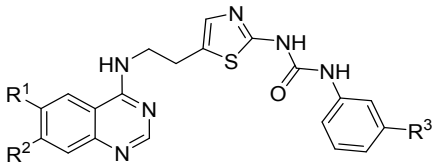

compound no.	R^1	R^2	R^3	RLMS (%)	Aurora A IC_{50} (nM)	Aurora B @ 100 nM	HCT-116 CC_{50} (nM)	Detroit 551 CC_{50} (μM)	Selectivity (Detroit 551/HCT-116 CC_{50})
1	H	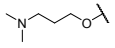	Cl	14.5	22	IC_{50} = 13 nM	141	4.0	29
22	H	H	Cl	80.4	15.0	71%	10.0	6.6	660
23	H	H	H	90.0	11.1	53%	29.0	17.0	586

24	H	OMe	H	41.8	18.8	74%	21.7	7.6	350
25	H	OEt	H	60.5	14.0	75%	17.7	6.7	379
26	H	Cl	H	67.3	24.0	50%	23.0	14.1	613
27	H	F	H	80.7	13.0	50%	66.0	16.1	244
28	H	CF_3	H	41.3	46.0	32%	229.2	8.6	38
29	F	H	H	71.1	14.0	52%	79.4	> 20	> 252
30	F	OMe	H	42.0	4.2	73%	21.2	5.8	274
31	F	OEt	H	47.4	12.0	69%	22.4	6.5	290
32	F	F	H	71.1	39.0	35%	83.2	> 20	> 240
33	H	OMe	Cl	77.5	9.0	89%	30.4	2.9	95
34	H	F	Cl	77.8	9.0	83% (IC_{50}	16.0	14.5	906

						= 30.5 nM)			
35	F	H	Cl	78.9	19.1	67%	23.0	14.7	639
36	F	F	Cl	87.7	13.3	45%	22.8	12.8	561
37	F	OEt	Cl	74.5	8.4	80% (IC_{50} = 64 nM)	52.0	4.5	87

[a]The rat liver microsomal stability (RLMS) assays offer a method to evaluate the rate of hepatic metabolism of a compound in liver microsomal incubation. Data was represented as % remaining at 30 min by incubation of the compound in rate microsomes.; [b]IC_{50} values represent the mean of at least two independent experiments.

Table 3. The physicochemical properties (PCPs) of the synthesized inhibitors[a].

compound no.	cLogP	MW	HBA	HBD	NRB	PSA	PCPs violations[b]
BPR1K871 (1)	4.2	526.1	9	3	11	132.54	2
8	3.9	513.0	9	3	11	138.53	2
11	3.0	576.1	11	4	12	183.85	4
12	3.2	540.0	10	4	11	158.39	3
16	4.1	538.1	9	3	8	132.54	1
17	4.1	482.0	8	3	8	123.3	0
18	3.8	511.0	9	3	8	138.53	1
19	4.0	525.0	9	3	9	138.52	1
20	4.4	544.0	9	3	11	132.54	2
21	4.2	543.0	9	3	9	138.53	1
22	4.0	424.9	7	3	6	120.07	0
23	3.3	390.5	7	3	6	120.07	0
24	3.3	420.5	8	3	7	129.3	0
25	3.7	434.5	8	3	8	129.3	0
26	4.0	424.9	7	3	6	120.07	0
27	3.5	408.5	7	3	6	120.07	0
28	4.3	458.5	7	3	7	120.07	0
29	3.5	408.5	7	3	6	120.07	0
30	3.5	438.5	8	3	7	129.29	0
31	3.9	452.5	8	3	8	129.29	0
32	3.7	426.4	7	3	6	120.07	0
33	4.0	454.9	8	3	7	129.29	0
34	4.2	442.9	7	3	6	120.07	0
35	4.2	442.9	7	3	6	120.07	0
36	4.4	460.9	7	3	6	120.07	0
37	4.5	487.0	8	3	8	129.29	0
41	4.2	556.1	10	3	12	141.77	3

[a]MW (molecular weight), cLogP (calculated LogP), HBA (number of hydrogen bond acceptors), HBD (number of hydrogen bond donors), NRB (number of free rotatable bond) and PSA (polar surface area) were calculated by using Discovery Studio.; [b]Violations according to the Lipinski's rule of five and Veber's suggestion.

Table 4. Pharmacokinetics profile of selected compounds in rat[a].

compound no.	IV (Dose: 5 mg/kg)				PO (Dose: 20 mg/kg)				F (%)
	$t_{1/2}$ (h)	CL (ml/min/kg)	V_{ss} (l/kg)	$AUC_{(0\text{-inf})}$ (ng/mL*h)	$t_{1/2}$ (h)	C_{max} (ng/mL)	T_{max} (h)	$AUC_{(0\text{-inf})}$ (ng/mL*h)	
1	23.5	60.4	34.2	1464	N.D.[a]	N.D.	N.D.	N.D.	N.D.
20	11.4	42.6	12.6	1958	N.D.	N.D.	N.D.	N.D.	N.D.
21	1.7	27.1	3.5	3272	2.8	125	5.3	818	6.3
22	4.6	52.5	5.7	1599	5.1	488	0.8	1951	30.0
23	1.3	61.7	4.0	1396	2.7	679	1.0	3014	46.0
27	6.8	24.3	3.2	3478	4.9	1111	0.7	2768	19.9
34	3.6	13.0	1.1	7451	3	4146	3.3	16065	54.0

[a]N.D.: Not determined.

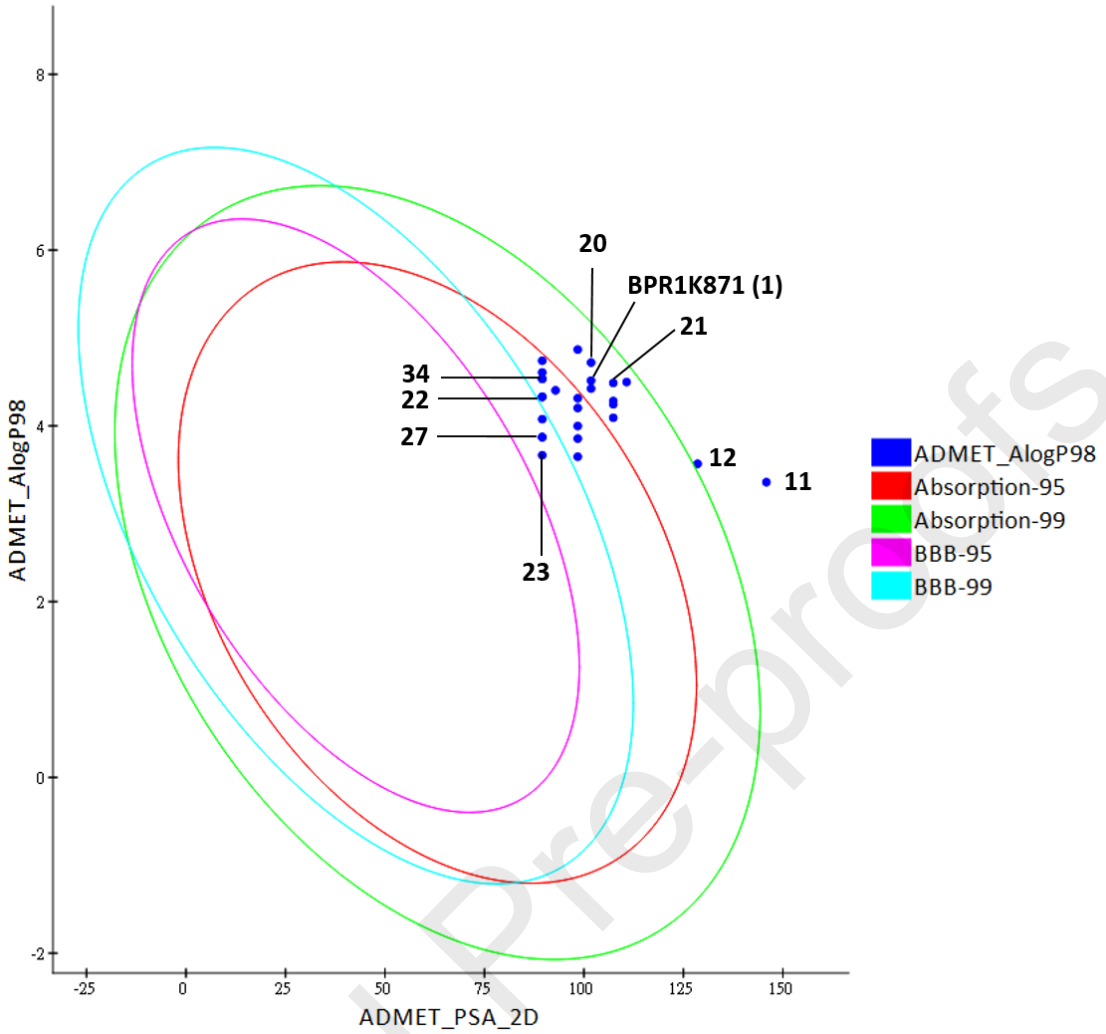

Figure 3. ADMET properties predicted for the quinazoline compounds. Compounds located inside the 95% confidence ellipse are better for this parameter.

Profiling of compound 34 in kinase panel and cancer cell lines

Based on the *in vitro* biological activities and *in vivo* PK data, compound **34** was selected as suitable candidate to further subject it to kinase profiling using the KINOME*scan* technology against a panel of 468 kinases (containing 403 non-mutant kinases) at a concentration of 100 nM (**Figure 4**) [36]. The results for binding

interactions were reported as %control. Inhibitor **34** displayed broad and high inhibition against several oncogenic kinases, such as Aurora kinase (2.5–14%), DDR1 (2.7%), DDR2 (7.6%), FLT3 (10%), HIPK4 (8.9%), KIT (20%), MERTK (18%), MKNK2 (6.7%), and TRK family (4.7–12%). Based on the profile, the compound **34** IC_{50}s for these kinases were evaluated by KINOME*scan* platform (**Figure 5**). Aurora kinase family members were potently inhibited at single-digit nanomolar concentrations of **34**. In addition, **34** demonstrated high potency (IC_{50}) against several kinases especially the tyrosine kinases, including FLT3 (129 nM), DDR1 (16.7 nM), DDR2 (143 nM), TRKA (23.6 nM), TRKB (35.5 nM), and TRKC (12.5 nM). These results overall suggested that **34** is a potent multi-kinase inhibitor.

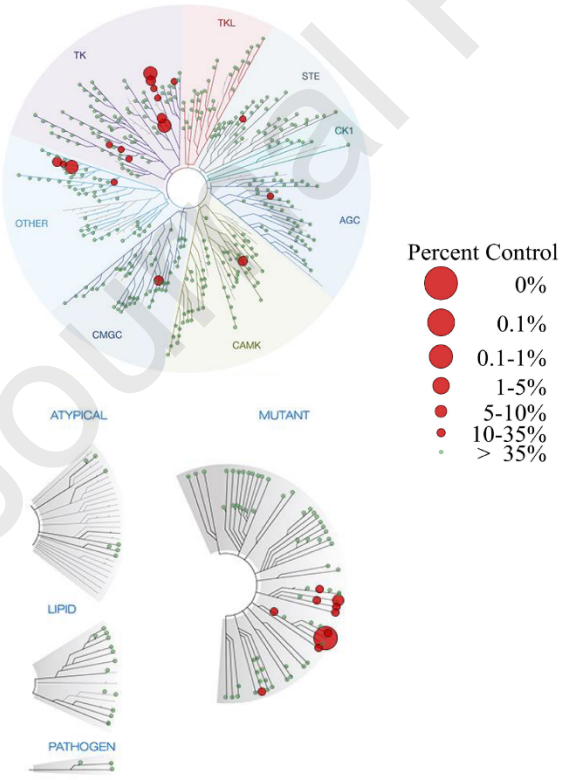

Figure 4. Kinase profiling of 34 using the KINOME*scan* technology.

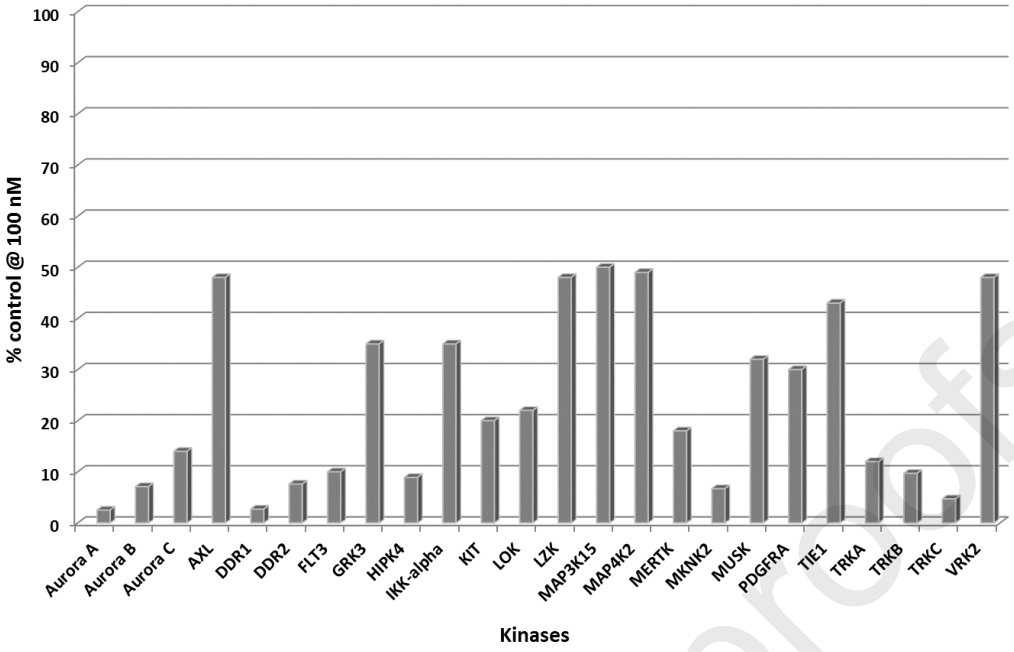

Figure 5. KINOME*scan* profile of compound **34** at 100 nM for kinases with % control < 50.

Next, **34** was tested in a panel of in-house cancer cell lines, including human colon cancer (Colo205, HCT-116), uterine sarcoma (MESSA), human gastric cancer (MKN-45), human lung cancer (H1975, H446), and acute myeloid leukemia (MOLM-13, MV4-11). For comparison, the two known multi-kinase inhibitors, linifanib and sorafenib, were also examined side-by-side. The results revealed that compound **34** showed better potency against colon cancer HCT-116 and leukemia cell lines MOLM-13 and MV4-11 (**Table 5**). **34** was more potent than the clinical candidate **1** in HCT-116 colon cancer and MKN45 human gastric cancer cell line; but was less potent in the case of leukemia cell lines MOLM-13, MV4-11, which harbor FLT3 mutations.

Table 5. Anti-proliferative activity of compound **34** in a panel of in-house cell lines.

compound no.	Cell lines CC_{50} (nM)								
	Solid tumor type						*Leukemia type*		*Normal type*
	Colo 205	HCT-116	MESSA	MKN45	H1975	H446	MOLM-13	MV4-11	Detroit 551
1 (BPR1K871)	34	141	216	355	495	–	5	4	4000
34	144	16	506	128	491	102	76	73	14500
Sorafenib	–	8800	–	–	7010	–	82	43	–
Linifanib	–	8070	–	–	8853	–	38	82	–

4. Conclusion

Discovering a new drug, particularly drugs that can be orally administered to patients is a challenging task. Nevertheless, orally administered drugs have the advantage of easy administration as compared to injectable forms. Administering a drug through oral route requires that the molecule be orally bioavailable, i.e., get absorbed through the gut and enter the systemic circulation without being extensively

metabolized in the liver. Means to manipulate and improve the oral bioavailability of a drug without compromising the activity is pursued during lead optimization stage.

In this respect, here we report our efforts to optimize our previous lead BPR1K871 (**1**), which is a clinical candidate for cancer treatment, to improve the pharmacokinetics property and identify orally bioavailable lead. Careful consideration of physicochemical properties (PCP) and *in vitro* rat liver microsomal stability (RLMS) data provided a path to carry out a systematic medicinal chemistry optimization of lead **1**. During PCP driven optimization it was found that the solubilizing functional group at the 7-position of quinazoline ring was not essential for maintaining the activity and also the group is responsible for poor metabolic stability and oral absorption. A detailed structural investigation at the 6- and 7-position of quinazoline ring identified **34** as an orally bioavailable multi-kinase inhibitor with *in vitro* enzyme/cellular activity profile very similar to lead **1**. The results suggest that **34** is a promising lead candidate for further evaluation of antitumor efficacy in animal models.

5. Experimental

5.1. Synthesis

5.1.1. General methods

All reagents were purchased from commercial suppliers and were used without further purification unless otherwise noted. All reactions were carried out under dry nitrogen or argon atmosphere and were monitored by TLC using Merck 60 F254 silica gel glass backed plates; zones were detected visually under UV irradiation (254 nm) or by spraying with phosphomolybdic acid reagent (Sigma-Aldrich) followed by heating at 80 °C. Flash column chromatography using silica gel (Merck Kiesegel 60, no. 9385, 230–400 mesh ASTM). ^{1}H NMR spectra were recorded on a Varian Mercury-300 or Varian Mercury-400 spectrometers, and the chemical shifts were recorded in parts per million (ppm, δ) and reported relative to TMS or the solvent peak. Low-resolution mass spectra (LRMS) data were obtained from Agilent MSD-1100 ESI-MS/ MS system and Agilent 1200 series APCI-ESI-MS/MS system. Purity of the final compounds were determined with a Hitachi 2000 series HPLC system using C-18 column (Agilent ZORBAX Eclipse XDB-C18 5 μm. 4.6 mm × 150 mm) operating at 25 °C. For method A, elution was carried out using water containing 0.1% formic acid + 10 mmol NH_4OAc as mobile phase A, and acetonitrile as mobile phase B. Elution conditions: 0 to 45 min, 10 to 90% mobile B; 45 to 60 min, 90% to 10% mobile B. For method B,

elution was carried out using water containing 0.1% formic acid + 2 mmol NH_4OAc as mobile phase A, and acetonitrile as mobile phase B. Elution conditions: 0 to 30 min, 10 to 90% mobile B; 30 to 37 min, 90% to 10% mobile B. The flow-rate of the mobile phase was 0.5 mL/min and the injection volume of the sample was 10 or 20 μL. Peaks were detected at 254 nm. IUPAC nomenclature of compounds were obtained with the software ACD/Name Pro.

*5.1.2. 1-(3-Chlorophenyl)-3-[5-(2-{[7-(3-methoxypropoxy)quinazolin-4-yl]amino}-ethyl)-1,3-thiazol-2-yl]urea (**8**).*

A mixture of compound **7** [18] (81.2 mg, 0.16 mmol, 1.0 equiv), and potassium iodide (81 mg, 0.48 mmol, 3.0 equiv) in anhydrous DMF (1 mL) was added 5M NaOMe in MeOH (0.13 ml, 0.64 mmol, 4.0 equiv). The mixture was heated at 100 °C for 16 h, then quenched with water and extracted with ethyl acetate. The organic layer was dried by anhydrous $MgSO_4$ then concentrated under vacuum. The crude was purified by silica gel column chromatography ($MeOH/CH_2Cl_2/NH_4OH$, 1:20:0.1) to give compound **8** as yellow solid (28 mg, 34%). ^1H NMR (400 MHz, DMSO-d_6) δ 10.54 (br s, 1H), 9.24 (br s, 1H), 8.42 (s, 1H), 8.27 (t, J = 6.4 Hz, 1H), 8.11 (d, J = 8.8 Hz, 1H), 7.69 (s, 1H), 7.32–7.30 (m, 2H), 7.14–7.05 (m, 4H), 4.15 (t, J = 6.4 Hz, 2H), 3.71 (q, J = 6.0 Hz, 2H), 3.50 (t, J = 6.4 Hz, 2H), 3.37 (s, 3H), 3.06 (t, J = 6.0 Hz, 2H), 2.00 (quint, J = 6.4 Hz, 2H); LRMS (ESI) m/z calcd for $C_{24}H_{25}ClN_6O_3S$, 512.14; found, 513.1 $[M + H]^+$;

HPLC purity (method A): 91.29%, t_R = 24.13 min.

*5.1.3. 1-[5-(2-{[7-(3-Azidopropoxy)quinazolin-4-yl]amino}ethyl)-1,3-thiazol-2-yl]-3-(3-chlorophenyl)urea (**9**).*

A mixture of compound **7** (30 mg, 0.058 mmol, 1.0 equiv) and sodium azide (4.7 mg, 0.072 mmol, 1.2 equiv) in DMSO (0.50 mL) was heated at 60 °C for 16 h. The mixture was quenched with water and then extracted with ethyl acetate. The organic layer was dried by anhydrous $MgSO_4$ then concentrated under vacuum. The crude was purified by silica gel column chromatography ($MeOH/CH_2Cl_2/NH_4OH$, 1:15:0.1) to give compound **9** as white solid (29 mg, 95%). ^{1}H NMR (400 MHz, DMSO-d_6) δ 10.45 (br s, 1H), 9.14 (br s, 1H), 8.42 (s, 1H), 8.28 (t, J = 5.6 Hz, 1H), 8.13 (d, J = 8.4 Hz, 1H), 7.69 (s, 1H), 7.33–7.25 (m, 2H), 7.15–7.00 (m, 4H), 4.18 (t, J = 6.0 Hz, 2H), 3.72 (q, J = 6.4 Hz, 2H), 3.54 (t, J = 6.4 Hz, 2H), 3.12–3.01 (m, 2H), 2.03 (tt, J = 6.4, 6.0 Hz, 2H); LRMS (ESI) m/z calcd for $C_{23}H_{22}ClN_9O_2S$, 523.13; found, 524.1 $[M+H]^+$.

*5.1.4. 1-[5-(2-{[7-(3-Aminopropoxy)quinazolin-4-yl]amino}ethyl)-1,3-thiazol-2-yl]-3-(3-chlorophenyl)urea (**10**).*

A mixture of **9** (99 mg, 0.19 mmol) and 5% Pd/C (17 mg) in MeOH (8.0 mL) was hydrogenated at atmospheric pressure and room temperature for 16 h. The reaction mixture was filtered over celite, and the solvents removed under vacuum to give the desired compound **10** (60 mg, 64%). ^{1}H NMR (400 MHz, DMSO-d_6) δ 9.80–9.40 (br,

1H), 8.41 (s, 1H), 8.26 (t, *J* =5.6 Hz, 1H), 8.11 (d, *J* = 9.2 Hz, 1H), 7.72 (s, 1H), 7.32–7.26 (m, 2H), 7.12–7.02 (m, 4H), 5.90–5.20 (br, 2H), 4.16 (t, *J* = 6.4 Hz, 2H), 3.72 (q, *J* = 7.2 Hz, 2H), 3.06 (t, *J* = 7.2 Hz, 2H), 2.76 (td, *J* =6.8, 1.6 Hz, 2H), 1.87 (tt, *J* = 6.8, 6.4 Hz, 2H); LRMS (ESI) m/z calcd for $C_{23}H_{24}ClN_7O2_S$, 497.14; found, 498.1 $[M+H]^+$.

*5.1.5. N-{3-[(4-{[2-(2-{[(3-Chlorophenyl)carbamoyl]amino}-1,3-thiazol-5-yl)ethyl-]amino}quinazolin-7-yl)oxy]propyl}methanesulfonamide (**11**).*

To a mixture of compound **10** (43 mg, 0.084 mmol, 1.0 equiv) and triethylamine (17.2 mg, 0.17 mmol, 2.0 equiv) in CH_2Cl_2 (1.0 mL) was added methanesulfonyl chloride (9.9 mg, 0.086 mmol, 1.0 equiv) and DMF (0.10 mL). The reaction mixture was then stirred at room temperature for 16 h. The reaction mixture was concentrated under vacuum, and then purified by silica gel column chromatography ($MeOH/CH_2Cl_2/NH_4OH$, 1:8:0.1) to give **11** as light yellow solid (7.6 mg, 15%). ^1H NMR (400 MHz, Acetone-d_6) δ 10.00–9.80 (br, 1H), 9.30–9.10 (br, 1H), 8.48 (s, 1H), 8.03 (d, *J* = 9.2 Hz, 1H), 7.82 (s, 1H), 7.61 (br s, 1H), 7.40 (dd, *J* = 8.0, 1.2 Hz, 1H), 7.31 (dd, *J* = 8.0, 8.0 Hz, 1H), 7.14–7.04 (m, 4H), 6.16 (br s, 1H), 4.26 (t, *J* = 6.0 Hz, 2H), 3.89 (q, *J* = 6.4 Hz, 2H), 3.36 (q, *J* = 6.4 Hz, 2H), 3.18 (t, *J* = 6.4 Hz, 2H), 2.92 (s, 3H), 2.13 (quint, *J* = 6.4 Hz, 2H); LRMS (ESI) m/z calcd for $C_{24}H_{26}ClN_7O_4S_2$, 575.12; found, 576.2 $[M + H]^+$; HPLC Purity (method A): 97.09%, t_R = 22.69 min.

5.1.6. N-{3-[(4-{[2-(2-{[(3-Chlorophenyl)carbamoyl]amino}-1,3-thiazol-5-yl)ethyl]-

*amino}quinazolin-7-yl)oxy]propyl}acetamide (**12**).*

To a mixture of compound **10** (80 mg, 0.16 mmol, 1.0 equiv) in CH_2Cl_2 (2.0 mL) was added pyridine (16 mg, 0.20 mmol, 1.3 equiv) and acetic anhydride (21 mg, 0.21 mmol, 1.3 equiv). The reaction mixture was then stirred at room temperature for 48 h. The reaction mixture was concentrated under vacuum, and then purified by silica gel column chromatography ($MeOH/CH_2Cl_2/NH_4OH$, 1:9:0.1) to give **12** as light yellow solid (31 mg, 35%). ^1H NMR (400 MHz, DMSO-d_6) δ 11.20–10.60 (br, 1H), 9.20 (br s, 1H), 8.56 (br s, 1H), 8.50 (s, 1H) , 8.16 (d, J = 8.8 Hz, 1H), 7.94 (t, J = 5.6 Hz, 1H), 7.69 (s, 1H), 7.31–7.30 (m, 2H), 7.17 (dd, J = 8.8, 2.4 Hz, 1H), 7.12 (s, 1H), 7.07–7.04 (m, 2H), 4.12 (t, J = 6.0 Hz, 2H), 3.78–3.73 (m, 2H), 3.21 (q, J = 6.8 Hz, 2H), 3.08 (t, J = 6.8 Hz, 2H), 1.92–1.85 (m, 2H), 1.80 (s, 3H); LRMS (ESI) m/z calcd for $C_{25}H_{26}ClN_7O_3S$, 539.15; found, 540.1 $[M + H]^+$; HPLC Purity (method A): 97.68%, t_R = 20.56 min.

*5.1.7. Standard procedure A for the synthesis of urea derivatives **16**–**37**.*

The amine derivative **15a**–**p** in a mixture of methanol (0.30–10 mL) and CH_2Cl_2 (2.5–150 mL) was treated with 3-chlorophenyl isocyanate or phenyl isocyanate, and the mixture was stirred at room temperature for 16 h. The reaction mixture was concentrated under reduced pressure to give a residue, which was purified using silica gel column chromatography to give the desired product in 6−99% yield.

5.1.8. 1-(3-Chlorophenyl)-3-{5-[2-({7-[(1-methylpiperidin-4-yl)oxy]quinazolin-4-

*yl}amino)ethyl]-1,3-thiazol-2-yl}urea (**16**).*

Following standard procedure A, **15a** (6.6 mg, 0.017 mmol, 1.0 equiv), 3-chlorophenyl isocyanate (31 μL, 0.22 mmol, 13 equiv), CH_2Cl_2 (10 mL), and methanol (0.50 mL) were used to carry out the reaction. After worked-up, **16** (9.2 mg, 99%) was obtained. ^{1}H-NMR (300 MHz, DMSO-d_6) δ 10.80–10.40 (br, 1H), 9.23 (br s, 1H), 8.41 (s, 1H), 8.26 (t, J = 5.4 Hz, 1H), 8.11 (d, J = 9.0 Hz, 1H), 7.69 (s, 1H), 7.31–7.30 (m, 2H), 7.14–7.04 (m, 4H), 4.62–4.57 (br m, 1H), 3.75–3.71 (m, 2H), 3.06 (t, J = 6.6 Hz, 2H), 2.64–2.60 (m, 2H), 2.38–2.23 (m, 5H), 2.05–1.90 (m, 2H), 1.78–1.68 (m, 2H); LRMS (ESI) m/z calcd for $C_{26}H_{28}ClN_7O_2S$, 537.17; found, 538.2 $[M + H]^+$; HPLC Purity (method A): 90.81%, t_R = 17.44 min.

*5.1.9. 1-(3-Chlorophenyl)-3-{5-[2-({7-[(dimethylamino)methyl]quinazolin-4-yl}amino)ethyl]-1,3-thiazol-2-yl}urea (**17**).*

Following standard procedure A, **15b** (260 mg, 0.792 mmol, 1.0 equiv), 3-chlorophenyl isocyanate (1.90 mL, 15.8 mmol, 20 equiv), and CH_2Cl_2 (10 mL) were used to carry out the reaction. After worked-up, **17** (128 mg, 34%) was obtained. ^{1}H NMR (400MHz, DMSO-d_6) δ 10.80–10.60 (br, 1H), 9.23 (br s, 1H), 8.46 (s, 1H), 8.38 (t, J = 5.6 Hz, 1H), 8.16 (d, J = 8.8 Hz, 1H), 7.69 (s, 1H), 7.55 (s, 1H), 7.45 (dd, J = 8.8, 1.6 Hz, 1H), 7.30 (s, 1H), 7.29 (s, 1H), 7.12 (s, 1H), 7.06–7.03 (m, 1H), 3.73 (q, J = 6.8 Hz, 2H), 3.52 (s, 2H), 3.07 (t, J = 6.8 Hz, 2H), 2.17 (s, 6H); LRMS (ESI) m/z calcd for

$C_{23}H_{24}ClN_7OS$, 481.15; found, 482.2 $[M + H]^+$; HPLC Purity (method A): 98.84%, t_R = 17.84 min.

*5.1.10. 1-(3-Chlorophenyl)-3-{5-[2-({7-[(3S)-tetrahydrofuran-3-yloxy]quinazolin-4-yl}amino)ethyl]-1,3-thiazol-2-yl}urea (**18**).*

Following standard procedure A, **15c** (258.7 mg, 0.7993 mmol, 1.0 equiv), 3-chlorophenyl isocyanate (0.75 mL, 6.2 mmol, 7.8 equiv), CH_2Cl_2 (10 mL), and methanol (0.50 mL) were used to carry out the reaction. After worked-up, **18** (346.8 mg, 85%) was obtained. ^{1}H-NMR (400 MHz, DMSO-d_6) δ 10.70–10.40 (br, 1H), 9.20 (br s, 1H), 8.42 (s, 1H), 8.27 (t, J = 5.2 Hz, 1H), 8.12 (d, J = 9.2 Hz, 1H), 7.70 (s, 1H), 7.34–7.30 (m, 2H), 7.12–7.05 (m, 4H), 5.24–5.20 (m, 1H), 3.95–3.70 (m, 6H), 3.06 (t, J = 6.4 Hz, 2H), 2.34–2.25 (m, 1H), 2.04–1.98 (m, 1H); LRMS (ESI) m/z calcd for $C_{24}H_{23}ClN_6O_3S$, 510.12; found, 511.2 $[M + H]^+$; HPLC Purity (method A): 99.25%, t_R = 22.85 min.

*5.1.11. 1-(3-Chlorophenyl)-3-[5-(2-{[7-(tetrahydrofuran-3-ylmethoxy)quinazolin-4-yl]amino}ethyl)-1,3-thiazol-2-yl]urea (**19**).*

Following standard procedure A, **15d** (77.4 mg, 0.208 mmol, 1.0 equiv), 3-chlorophenyl isocyanate (30 µL, 0.25 mmol, 1.2 equiv), and CH_2Cl_2 (10 mL) were used to carry out the reaction. After worked-up, **19** (103.2 mg, 94%) was obtained. ^{1}H-NMR

(400 MHz, DMSO-d_6) δ 10.70–10.30 (br, 1H), 9.15 (br s, 1H), 8.41 (s, 1H), 8.25 (t, J = 5.4 Hz, 1H), 8.12 (d, J = 8.8 Hz, 1H), 7.69 (s, 1H), 7.34–7.26 (m, 2H), 7.16–7.02 (m, 4H), 4.12–4.00 (m, 2H), 3.85–3.62 (m, 5H), 3.60–3.52 (m, 1H), 3.07 (t, J = 6.8 Hz, 2H), 2.75–2.63 (m, 1H), 2.10–1.99 (m, 1H), 1.73–1.63 (m, 1H);LRMS (ESI) m/z calcd for $C_{25}H_{25}ClN_6O_3S$, 524.14; found, 525.1 $[M + H]^+$; HPLC Purity (method B): 98.46%, t_R = 16.45 min.

*5.1.12. 1-(3-Chlorophenyl)-3-{5-[2-({7-[3-(dimethylamino)propoxy]-6-fluoro-quinazolin-4-yl}amino)ethyl]-1,3-thiazol-2-yl}urea (**20**).*

Following standard procedure A, **15e** (17 mg, 0.044 mmol, 1.0 equiv), 3-chlorophenyl isocyanate (16 μL, 0.13 mmol, 3.0 equiv), and CH_2Cl_2 (7.0 mL) were used to carry out the reaction. After worked-up, **20** (11.3 mg, 48%) was obtained. ^{1}H-NMR (300 MHz, DMSO-d_6) δ 10.80–10.50 (br, 1H), 9.35–9.10 (br, 1H), 8.43 (s, 1H), 8.16 (t, J = 5.6 Hz, 1H), 8.08 (d, J = 12.0 Hz, 1H), 7.71 (s, 1H), 7.34–7.25 (m, 3H), 7.10 (s, 1H), 7.04–7.02 (m, 1H), 4.20 (t, J = 6.0 Hz, 2H), 3.72–3.69 (m, 2H), 3.05 (t, J = 6.9 Hz, 2H), 2.38 (t, J = 6.9 Hz, 2H), 2.13 (s, 6H), 1.91 (quintet, J = 6.9 Hz, 2H); LRMS (ESI) m/z calcd for $C_{25}H_{27}ClFN_7O_2S$, 543.16; found, 544.2 $[M + H]^+$; HPLC Purity (method B): 96.68%, t_R = 14.16 min.

*5.1.13. 1-(3-Chlorophenyl)-3-[5-(2-{[6-fluoro-7-(tetrahydrofuran-3-ylmethoxy)quinazolin-4-yl]amino}ethyl)-1,3-thiazol-2-yl]urea (**21**).*

Following standard procedure A, **15f** (90.0 mg, 0.231 mmol, 1.0 equiv), 3-chlorophenyl isocyanate (112 μL, 0.926 mmol, 4.0 equiv), and CH_2Cl_2 (10 mL) were used to carry out the reaction. After worked-up, **21** (99.6 mg, 79%) was obtained. ^{1}H-NMR (400 MHz, DMSO-d_6) δ 10.90–10.60 (br, 1H), 9.30 (br s, 1H), 8.44 (s, 1H), 8.17 (t, J = 5.6 Hz, 1H), 8.08 (d, J = 12.4 Hz, 1H), 7.70 (s, 1H), 7.34–7.26 (m, 3H), 7.12 (s, 1H), 7.09–7.02 (m, 1H), 4.20–4.08 (m, 2H), 3.83–3.64 (m, 5H), 3.59–3.53 (m, 1H), 3.06 (t, J = 6.8 Hz, 2H), 2.80–2.69 (m, 1H), 2.10–2.00 (m, 1H), 1.76–1.68 (m, 1H); LRMS (ESI) m/z calcd for $C_{25}H_{24}ClFN_6O_3S$, 542.13; found, 543.1 $[M + H]^+$;HPLC Purity (method B): 99.62%, t_R = 18.25 min.

*5.1.14. 1-(3-Chlorophenyl)-3-{5-[2-(quinazolin-4-ylamino)ethyl]-1,3-thiazol-2-yl}urea (**22**).*

Following standard procedure A, **15g** (100 mg, 0.369 mmol, 1.0 equiv), 3-chlorophenyl isocyanate (0.90 mL, 7.37 mmol, 20 equiv), CH_2Cl_2 (20 mL), and methanol (0.50 mL) were used to carry out the reaction. After worked-up, **22** (81 mg, 52%) was obtained. ^{1}H-NMR (300 MHz, DMSO-d_6) δ 10.43 (br s, 1H), 9.13 (br s, 1H), 8.48 (s, 1H), 8.43 (t, J = 4.8 Hz, 1H), 8.20 (d, J = 7.5 Hz, 1H), 7.76–7.66 (m, 3H), 7.54–7.49 (m, 1H), 7.30–7.29 (m, 2H), 7.12 (s, 1H), 7.07–7.04 (m, 1H), 3.75 (q, J = 6.6 Hz, 2H), 3.08 (t, J =6.6 Hz, 2H). LRMS (ESI) m/z calcd for $C_{20}H_{17}ClN_6OS$, 424.09; found, 425.1 $[M + H]^+$. HPLC Purity (method A): 96.03%, t_R = 22.06 min.

*5.1.15. 1-Phenyl-3-{5-[2-(quinazolin-4-ylamino)ethyl]-1,3-thiazol-2-yl}urea (**23**).*

Following standard procedure A, **15g** (76 mg, 0.28 mmol, 1.0 equiv), phenyl isocyanate (0.30 mL, 2.8 mmol, 10 equiv), and CH_2Cl_2 (20 mL) were used to carry out the reaction. After worked-up, **23** (67 mg, 61%) was obtained. ^{1}H-NMR (300 MHz, DMSO-d_6) δ 10.50–10.30 (br, 1H), 8.98 (br s, 1H), 8.48 (s, 1H), 8.42 (t, J = 5.7 Hz, 1H), 8.21 (d, J = 8.1 Hz, 1H), 7.80–7.67 (m, 2H), 7.54–7.43 (m, 3H), 7.29 (dd, J = 8.4, 7.6 Hz, 2H), 7.12 (s, 1H), 7.01 (t, J = 7.6 Hz, 1H), 3.76 (q, J = 6.4 Hz, 2H), 3.10 (t, J = 6.4 Hz, 2H); LRMS (ESI) m/z calcd for $C_{20}H_{18}N_6OS$, 390.13; found, 391.1 $[M + H]^+$; HPLC Purity (method A): 99.54%, t_R = 18.44 min.

*5.1.16. 1-(5-{2-[(7-Methoxyquinazolin-4-yl)amino]ethyl}-1,3-thiazol-2-yl)-3-phenylurea (**24**).*

Following standard procedure A, **15h** (100 mg, 0.332 mmol, 1.0 equiv), phenyl isocyanate (54 μL, 0.50 mmol, 1.5 equiv), and CH_2Cl_2 (10 mL) were used to carry out the reaction. After worked-up, **24** (117 mg, 84%) was obtained. ^{1}H-NMR (400 MHz, DMSO-d_6) δ 10.35 (br s, 1H), 8.97 (br s, 1H), 8.42 (s, 1H), 8.27 (t, J = 5.6 Hz, 1H), 8.11 (d, J = 9.2 Hz, 1H), 7.45 (d, J = 7.6 Hz, 2H), 7.30 (dd, J = 8.0, 7.6 Hz, 2H), 7.13–7.05 (m, 3H), 7.01 (t, J = 7.6 Hz, 1H), 3.88 (s, 3H), 3.72 (q, J = 6.8 Hz, 2H), 3.08 (t, J = 6.8 Hz, 2H); LRMS (ESI) m/z calcd for $C_{21}H_{20}N_6O_2S$, 420.14; found, 421.2 [M + H]

$^{+}$; HPLC Purity (method B): 99.71%, t_R = 14.23 min.

*5.1.17. 1-(5-{2-[(7-Ethoxyquinazolin-4-yl)amino]ethyl}-1,3-thiazol-2-yl)-3-phenylurea (**25**).*

Following standard procedure A, **15i** (100 mg, 0.317 mmol, 1.0 equiv), phenyl isocyanate (0.30 mL, 3.2 mmol, 10 equiv), and CH_2Cl_2 (10 mL) were used to carry out the reaction. After worked-up, **25** (8.0 mg, 6%) was obtained.^{1}H-NMR (400 MHz, DMSO-d_6) δ 10.44 (br s, 1H), 9.01 (br s, 1H), 8.41 (s, 1H), 8.24 (t, J = 5.6 Hz, 1H), 8.11 (d, J = 8.8 Hz, 1H), 7.45 (d, J = 8.4 Hz, 2H), 7.29 (dd, J = 7.6. 7.6 Hz, 2H), 7.11–6.99 (m, 4H), 4.15 (q, J = 6.8 Hz, 2H), 3.72 (q, J = 6.8 Hz, 2H), 3.07 (t, J = 6.8 Hz, 2H), 1.37 (t, J = 6.8Hz, 3H); LRMS (ESI) m/z calcd for $C_{22}H_{22}N_6O_2S$, 434.15; found, 435.1 $[M + H]^+$; HPLC Purity (method A): 93.63%, t_R = 22.22 min.

*5.1.18. 1-(5-{2-[(7-Chloroquinazolin-4-yl)amino]ethyl}-1,3-thiazol-2-yl)-3-phenylurea (**26**).*

Following standard procedure A, **15j** (100 mg, 0.327 mmol, 1.0 equiv), phenyl isocyanate (0.20 mL, 1.6 mmol, 5.0 equiv), and CH_2Cl_2 (5.0 mL) were used to carry out the reaction. After worked-up, **26** (130 mg, 94%) was obtained. ^{1}H-NMR (300 MHz, DMSO-d_6) δ 10.41 (br s, 1H), 9.00 (br s, 1H), 8.58 (br t, 1H), 8.47 (s, 1H), 8.23 (d, J = 8.7 Hz, 1H), 7.72 (s, 1H), 7.57 (d, J = 8.7 Hz, 1H), 7.44 (d, J = 7.8 Hz, 2H), 7.29 (dd, J = 7.8, 7.5 Hz, 2H), 7.11 (s, 1H), 7.01 (t, J = 6.9 Hz, 1H), 3.76–3.65 (m, 2H), 3.15–

3.08 (m, 2H); LRMS (ESI) m/z calcd for $C_{20}H_{17}ClN_6OS$, 424.09; found, 425.0 [M + H]$^+$; HPLC Purity (method A): 99.79%, t_R = 23.90 min.

*5.1.19. 1-(5-{2-[(7-Fluoroquinazolin-4-yl)amino]ethyl}-1,3-thiazol-2-yl)-3-phenyl-urea (**27**).*

Following standard procedure A, **15k** (129 mg, 0.45 mmol, 1.0 equiv), phenyl isocyanate (0.49 mL, 4.5 mmol, 10 equiv), and CH_2Cl_2 (20 mL) were used to carry out the reaction. After worked-up, **27** (52 mg, 29%) was obtained. ^{1}H-NMR (400 MHz, DMSO-d_6) δ 10.64 (br s, 1H), 9.18 (br s, 1H), 8.52 (br t, 1H), 8.48 (s, 1H), 8.33–8.30 (m, 1H), 7.45–7.40 (m, 4H), 7.28 (dd, J =7.2, 7.2 Hz, 2H), 7.11 (s, 1H), 7.00 (t, J =7.2 Hz, 1H), 3.75 (q, J =6.4 Hz, 2H), 3.08 (t, J =6.4 Hz, 2H); LRMS (ESI) m/z calcd for $C_{20}H_{17}FN_6OS$, 408.12; found, 409.1 [M + H] $^+$; HPLC Purity (method A): 97.04%, t_R = 20.93 min.

*5.1.20. 1-Phenyl-3-[5-(2-{[7-(trifluoromethyl)quinazolin-4-yl]amino}ethyl)-1,3-thiazol- 2-yl]urea (**28**).*

Following standard procedure A, **15l** (50.0 mg, 0.147 mmol, 1.0 equiv), phenyl isocyanate (0.20 mL, 1.6 mmol, 10 equiv), and CH_2Cl_2 (3.0 mL) were used to carry out the reaction. After worked-up, **28** (60 mg, 89%) was obtained. ^{1}H-NMR (300 MHz, DMSO-d_6) δ 10.34 (br s, 1H), 8.94 (br s, 1H), 8.77 (br t, 1H), 8.60 (s, 1H), 8.46 (d, J = 8.7 Hz, 1H), 8.01 (s, 1H), 7.85 (d, J = 8.7 Hz, 1H), 7.44 (d, J = 8.4 Hz, 2H), 7.29 (dd,

J = 8.4, 7.2 Hz, 2H), 7.12 (s, 1H), 7.01 (t, *J* = 7.2 Hz, 1H), 3.79–3.77 (m, 2H), 3.11 (t, *J* = 6.6 Hz, 2H); LRMS (ESI) m/z calcd for $C_{21}H_{17}F_3N_6OS$, 458.11; found, 459.1 [M + H]$^+$; HPLC Purity (method A): 99.84%, t_R = 29.03 min.

*5.1.21. 1-(5-{2-[(6-Fluoroquinazolin-4-yl)amino]ethyl}-1,3-thiazol-2-yl)-3-phenyl-urea (**29**).*

Following standard procedure A, **15m** (100 mg, 0.346 mmol, 1.0 equiv), phenyl isocyanate (0.40 mL, 3.46 mmol, 10 equiv), and CH_2Cl_2 (10 mL) were used to carry out the reaction. After worked-up, **29** (101 mg, 72%) was obtained. ^{1}H-NMR (300 MHz, DMSO-d_6) δ 10.45 (br s, 1H), 9.02 (br s, 1H), 8.49 (s, 1H), 8.39 (t, *J* = 5.4 Hz, 1H), 8.08 (dd, *J* = 9.9, 2.7 Hz, 1H), 7.79–7.65 (m, 2H), 7.45 (d, *J* = 8.1 Hz, 2H), 7.29 (dd, *J* = 8.1, 7.2 Hz, 2H), 7.12 (s, 1H), 7.01 (t, *J* = 7.2 Hz, 1H), 3.78–3.72 (m, 2H), 3.09 (t, *J* = 6.6 Hz, 2H). LRMS (ESI) m/z calcd for $C_{20}H_{17}FN_6OS$ 408.12; found, 409.1 [M + H]$^+$. HPLC Purity (method A): 100.0%, t_R = 21.25 min.

*5.1.22. 1-(5-{2-[(6-Fluoro-7-methoxyquinazolin-4-yl)amino]ethyl}-1,3-thiazol-2-yl)-3-phenylurea (**30**).*

Following standard procedure A, **15n** (100 mg, 0.313 mmol, 1.0 equiv), phenyl isocyanate (50 μL, 0.47 mmol, 1.5 equiv), and CH_2Cl_2 (10 mL) were used to carry out the reaction. After worked-up, **30** (63.8 mg, 47%) was obtained. ^{1}H-NMR (400 MHz, DMSO-d_6) δ 10.33 (br s, 1H), 8.94 (s, 1H), 8.44 (s, 1H), 8.18 (t, *J* = 5.4 Hz, 1H), 8.08

(d, J = 12.4 Hz, 1H), 7.44 (d, J = 8.0 Hz, 2H), 7.32–7.25 (m, 3H), 7.11 (s, 1H), 7.01 (t, J = 7.6 Hz, 1H), 3.97 (s, 3H), 3.72 (q, J = 6.8 Hz, 2H), 3.07 (t, J = 6.8 Hz, 2H); LRMS (ESI) m/z calcd for $C_{21}H_{19}FN_6O_2S$, 438.13; found, 439.2 $[M + H]^+$; HPLC Purity (method B): 99.56%, t_R = 14.76 min.

*5.1.23. 1-(5-{2-[(7-Ethoxy-6-fluoroquinazolin-4-yl)amino]ethyl}-1,3-thiazol-2-yl)-3-phenylurea (**31**).*

Following standard procedure A, **15o** (100 mg, 0.300 mmol, 1.0 equiv), phenyl isocyanate (0.30 mL, 3.0 mmol, 10 equiv), and CH_2Cl_2 (10 mL) were used to carry out the reaction. After worked-up, **31** (112 mg, 83%) was obtained. ^{1}H-NMR (400 MHz, DMSO-d_6) δ 10.42 (br s, 1H), 9.99 (br s, 1H), 8.43 (s, 1H), 8.17 (t, J = 5.2 Hz, 1H), 8.07 (d, J = 12.0 Hz, 1H), 7.45 (d, J = 8.0 Hz, 2H), 7.32–7.26 (m, 3H), 7.12 (s, 1H), 7.01 (t, J = 7.6 Hz, 1H), 4.24 (q, J = 6.8 Hz, 2H), 3.72 (q, J = 6.4 Hz, 2H), 3.07 (t, J = 6.4 Hz, 2H), 1.40 (t, J = 6.8 Hz, 3H); LRMS (ESI) m/z calcd for $C_{22}H_{21}FN_6O_2S$, 452.14; found, 453.1 $[M + H]^+$; HPLC Purity (method A): 100.00%, t_R = 23.09 min.

*5.1.24. 1-(5-{2-[(6,7-Difluoroquinazolin-4-yl)amino]ethyl}-1,3-thiazol-2-yl)-3-phenylurea (**32**).*

Following standard procedure A, **15p** (40.0 mg, 0.199 mmol, 1.0 equiv), phenyl isocyanate (0.11 mL, 1.0 mmol, 5.0 equiv), and CH_2Cl_2 (10 mL) were used to carry out the reaction. After worked-up, **32** (31.0 mg, 36%) was obtained. ^{1}H-NMR (400 MHz,

DMSO-d_6) δ 10.33 (br s, 1H), 8.95 (br s, 1H), 8.48 (s, 1H), 8.42 (t, J = 5.2 Hz, 1H), 8.32 (dd, J = 11.6, 8.8 Hz, 1H), 7.70 (dd, J = 11.6, 8.0 Hz, 1H), 7.43 (d, J = 8.0 Hz, 2H), 7.28 (dd, J = 8.0, 7.2 Hz, 2H), 7.10 (s, 1H), 6.99 (t, J = 7.2 Hz, 1H), 3.73 (q, J = 6.4 Hz, 2H), 3.06 (t, J = 6.4 Hz, 2H); LRMS (ESI) m/z calcd for $C_{20}H_{16}F_2N_6OS$, 426.11; found, 427.2 $[M + H]^+$; HPLC Purity (method B): 90.80%, t_R = 18.82 min.

*5.1.25. 1-(3-Chlorophenyl)-3-(5-{2-[(7-methoxyquinazolin-4-yl)amino]ethyl}-1,3-thiazol-2-yl)urea (**33**).*

Following standard procedure A, **15h** (50 mg, 0.17 mmol, 1.0 equiv), 3-chlorophenyl isocyanate (0.40 mL, 3.3 mmol, 20 equiv), and CH_2Cl_2 (20 mL) were used to carry out the reaction. After worked-up, **33** (25 mg, 33%) was obtained. ^{1}H NMR (400MHz, DMSO-d_6) δ 10.48 (br s, 1H), 9.18 (br s, 1H), 8.43 (s, 1H), 8.28 (t, J = 5.6 Hz, 1H), 8.11 (d, J = 9.2 Hz, 1H), 7.68 (s, 1H), 7.30–7.29 (m, 2H), 7.13–7.03 (m, 4H), 3.87 (s, 3H), 3.72 (q, J = 6.8 Hz, 2H), 3.06 (t, J = 6.8 Hz, 2H); LRMS (ESI) m/z calcd for $C_{21}H_{19}ClN_6O_2S$, 454.10; found, 455.1 $[M + H]^+$; HPLC Purity (method A): 95.88%, t_R = 22.76 min.

*5.1.26. 1-(3-Chlorophenyl)-3-(5-{2-[(7-fluoroquinazolin-4-yl)amino]ethyl}-1,3-thiazol-2-yl)urea (**34**).*

Following standard procedure A, **15k** (100 mg, 0.345 mmol, 1.0 equiv), 3-chlorophenyl isocyanate (0.40 mL, 3.5 mmol, 10 equiv), and CH_2Cl_2 (10 mL) were used to carry out

the reaction. After worked-up, **34** (113 mg, 74%) was obtained. ^{1}H-NMR (300 MHz, DMSO-d_6) δ 10.59 (br s, 1H), 9.22 (br s, 1H), 8.53 (t, J = 5.4 Hz, 1H), 8.49 (s, 1H), 8.31 (dd, J = 9.0, 8.8 Hz, 1H), 7.69 (s, 1H), 7.47–7.40 (m, 2H), 7.33–7.30 (m, 2H), 7.12 (s, 1H), 7.07–7.04 (m, 1H), 3.75 (q, J = 6.8 Hz, 2H), 3.08 (t, J = 6.8 Hz, 2H); LRMS (ESI) m/z calcd for $C_{20}H_{16}ClFN_6OS$, 442.08; found, 443.0 $[M + H]^+$; HPLC Purity (method A): 99.75 %, t_R = 25.13 min.

*5.1.27. 1-(3-Chlorophenyl)-3-(5-{2-[(6-fluoroquinazolin-4-yl)amino]ethyl}-1,3-thiazol-2-yl)urea (**35**).*

Following standard procedure A, **15m** (100 mg, 0.345 mmol, 1.0 equiv), 3-chlorophenyl isocyanate (63 µL, 0.52 mmol, 1.5 equiv), and CH_2Cl_2 (10 mL) were used to carry out the reaction. After worked-up, **35** (100 mg, 66%) was obtained. ^{1}H-NMR (300 MHz, DMSO-d_6) δ 10.49 (br s, 1H), 9.17 (br s, 1H), 8.76 (br s, 1H), 8.59 (s, 1H), 8.13 (dd, J = 9.9, 2.4 Hz, 1H), 7.83–7.68 (m, 3H), 7.34–7.28 (m, 2H), 7.14 (s, 1H), 7.10–7.02 (m, 1H), 3.79 (q, J = 6.6 Hz, 2H), 3.10 (t, J = 6.6 Hz, 2H); LRMS (ESI) m/z calcd for $C_{20}H_{16}ClFN_6OS$, 442.08; found, 443.1 $[M + H]^+$; HPLC Purity (method B): 99.70%, t_R = 15.69 min.

*5.1.28. 1-(3-Chlorophenyl)-3-(5-{2-[(6,7-difluoroquinazolin-4-yl)amino]ethyl}-1,3-thiazol-2-yl)urea (**36**).*

Following standard procedure A, **15p** (330 mg, 1.65 mmol, 1.0 equiv), 3-chlorophenyl

isocyanate (1.0 mL, 8.3 mmol, 5.0 equiv), and CH_2Cl_2 (10 mL) were used to carry out the reaction. After worked-up, **36** (395 mg, 59%) was obtained. ^{1}H-NMR (300 MHz, DMSO-d_6) δ 10.51 (br s, 1H), 9.16 (br s, 1H), 8.50 (s, 1H), 8.44 (t, J = 5.4 Hz, 1H), 8.33 (dd, J = 11.4, 8.7 Hz, 1H), 7.75–7.69 (m, 2H), 7.35–7.23 (m, 2H), 7.13 (s, 1H), 7.10–7.06 (m, 1H), 3.75 (q, J = 6.0, 2H), 3.07 (t, J = 6.0 Hz, 2H); LRMS (ESI) m/z calcd for $C_{20}H_{15}ClF_2N_6OS$, 460.07; found, 461.0 $[M + H]^+$; HPLC Purity (method B): 89.70%, t_R = 23.27 min.

*5.1.29. 1-(3-Chlorophenyl)-3-(5-{2-[(7-ethoxy-6-fluoroquinazolin-4-yl)amino]ethyl}-1,3-thiazol-2-yl)urea (**37**).*

Following standard procedure A, **15o** (45.0 mg, 0.199 mmol, 1.0 equiv), 3-chlorophenyl isocyanate (0.12 mL, 1.0 mmol, 5.0 equiv), and CH_2Cl_2 (10 mL) were used to carry out the reaction. After worked-up, **37** (53.5 mg, 55%) was obtained. ^{1}H-NMR (300 MHz, DMSO-d_6) δ 10.69 (br s, 1H), 9.27 (br s, 1H), 8.43 (s, 1H), 8.17 (t, J = 5.4 Hz, 1H), 8.07 (d, J = 12.6 Hz, 1H), 7.69 (s, 1H), 7.32–7.25 (m, 3H), 7.12 (s, 1H), 7.06–7.05 (m, 1H), 4.24 (q, J = 6.9 Hz, 2H), 3.72 (q, J = 6.6, 2H), 3.07 (t, J = 6.6 Hz, 2H), 1.41 (t, J = 6.9 Hz, 3H); LRMS (ESI) m/z calcd for $C_{22}H_{20}ClFN_6O_2S$, 486.10; found, 487.1 $[M + H]^+$. HPLC Purity (method A): 98.97%, t_R = 27.07 min.

*5.1.30. tert-Butyl[5-(2-{[7-(3-chloropropoxy)-6-methoxyquinazolin-4-yl]amino}ethyl)-1,3-thiazol-2-yl]carbamate (**39**).*

To a solution of 4-chloro-7-(3-chloropropoxy)-6-methoxyquinazoline **38** [24] (300 mg, 1.045 mmol, 1.0 equiv) and triethylamine (0.22 mL, 1.5 mmol, 1.4 equiv) in ethanol (15 mL) was added *tert*-butyl 5-(2-aminoethyl)thiazol-2-yl-carbamate (285 mg, 1.15 mmol, 1.1 equiv). The reaction mixture was stirred at reflux for 16 h, cooled to room temperature, and concentrated under reduced pressure. The residue was treated with dichloromethane and water. The collected organic layer was dried over $MgSO_4$, filtered, and concentrated to give a residue. The residue was purified by combiflash column chromatography ($MeOH/CH_2Cl_2$, 1:20 to 4:20) to give compound **39** as a solid product (400 mg, 78%); ^{1}H-NMR (400 MHz, DMSO-d_6) δ 11.25 (br s, 1H), 8.36 (s, 1H), 8.10 (t, J = 5.6 Hz, 1H), 7.59 (s, 1H), 7.11 (s, 2H), 4.22 (t, J = 6.0 Hz, 2H), 3.88 (s, 3H), 3.81 (t, J = 6.4 Hz, 2H), 3.71 (q, J = 6.8 Hz, 2H), 3.07 (t, J = 6.8 Hz, 2H), 2.23 (quintet, J = 6.4 Hz, 2H), 1.46 (s, 9H); LRMS (ESI) m/z calcd for $C_{22}H_{28}ClN_5O_4S$, 493.16; found, 494.1 $[M + H]^+$.

*5.1.31. 1-(3-Chlorophenyl)-3-[5-(2-{[7-(3-chloropropoxy)-6-methoxyquinazolin-4-yl]-amino}ethyl)-1,3-thiazol-2-yl]urea (**40**).*

A solution of compound **39** (400 mg, 0.810 mmol, 1.0 equiv) in trifluoroacetic acid (3.0 mL) and CH_2Cl_2 (15 mL) was stirred at room temperature for 2 h. The reaction mixture was concentrated and purified by combiflash column chromatography ($MeOH/CH_2Cl_2$, 1:6) to give the de-protected intermediate. The intermediate was dissolved in CH_2Cl_2

(25 mL) and methanol (1.0 mL), and then added 3-chlorophenyl isocyanate (4.40 mL, 36.4 mmol,). The reaction mixture was stirred for 16 h at room temperature and then concentrated to give a residue. The residue was purified by combiflash column chromatography ($MeOH/CH_2Cl_2$, 1:20 to 4:20) to give compound **40** as a solid (328 mg, 66%); ^{1}H-NMR (400 MHz, DMSO-d_6) δ 10.45 (br s, 1H), 9.14 (br s, 1H), 8.39 (s, 1H), 8.18 (br s, 1H), 7.69 (d, J = 8.0 Hz, 1H), 7.61 (s, 1H), 7.34–7.30 (m, 2H), 7.07–7.03 (m, 3H), 4.24 (t, J = 6.0 Hz, 2H), 3.94 (s, 3H), 3.91–3.77 (m, 4H), 3.09 (t, J = 6.8 Hz, 2H), 2.25 (quintet, J = 6.0 Hz, 2H); LRMS (ESI) m/z calcd for $C_{24}H_{24}Cl_2N_6O_3S$, 546.10; found, 547.1 $[M + H]^+$.

*5.1.32. 1-(3-Chlorophenyl)-3-{5-[2-({7-[3-(dimethylamino)propoxy]-6-methoxy-quinazolin-4-yl}amino)ethyl]-1,3-thiazol-2-yl}urea (**41**).*

To a solution of **40** (320 mg, 0.585 mmol, 1.0 equiv) in DMF (2.0 mL) was added 40% dimethylamine in water solution (1.32 g, 1.15 mmol, 2.0 equiv). The reaction mixture was stirred at reflux for 3 h and concentrated under vacuum. The residue was purified by combiflash column chromatography ($MeOH/CH_2Cl_2/NH_4OH$, 1:10:0.6) to give compound **41** as a solid (261 mg, 80%); ^{1}H-NMR (400 MHz, DMSO-d_6) δ 10.64 (br s, 1H), 9.17 (br s, 1H), 8.36 (s, 1H), 8.09 (t, J = 4.5 Hz, 1H), 7.70 (s, 1H), 7.57 (s 1H), 7.32–7.29 (m, 2H), 7.14 (s, 1H), 7.07–7.04 (m, 2H), 4.12 (t, J = 4.8 Hz, 2H), 3.88 (s, 3H), 3.73 (q, J = 5.1 Hz, 2H), 3.07 (t, J = 5.1 Hz, 2H), 2.38 (t, J = 5.1 Hz, 2H), 2.16 (s,

6H), 1.91 (quintet, J = 5.1 Hz, 2H). LRMS (ESI) m/z calcd for $C_{26}H_{30}ClN_7O_3S$, 555.18; found, 556.2 $[M + H]^+$; HPLC Purity (method A): 99.70%, t_R = 17.82 min.

5.2. Biology

5.2.1 Aurora A kinase inhibition assay

Aurora A kinase assay was conducted as previously described [18]. The recombinant GST–tAurora A (residues Ser123-Ser401) containing the kinase domain was expressed in Sf9 insect cells. The kinase assay was carried out in 96-well plates with tested compounds in a final volume of 50 μL at 37 °C for 90 min in Aur buffer (50 mM Tris-HCl pH 7.4, 10 mM NaCl, 10 mM MgCl2, 0.01% BSA) with 5.0 μM ATP, 1 mM DTT, 15 μM tetra(LRRASLG) peptide, and 150 ng recombinant Aurora A kinase. Kinase-Glo Plus Reagent was added to the reactions, followed by incubation at 25 °C for 20 min. The reactions were transferred to 96-well black plates (237108, NUNC) to quantify the ATP remaining in the solution. The luminescence was recorded by vector^2 V (1420 multilable HTS counter, Perkin-Elmer).

5.2.2 Aurora B kinase inhibition assay

Aurora B kinase assay was described similar with previous report [18]. The recombinant full length His-tagged Aurora-B (residues M1~A344) was obtained from Invitrogen (Catalog number: PV6130). The kinase assay was carried out in 96-well plates with a tested compound in reaction mixture (50 mM Tris-HCl pH 7.4, 10 mM

NaCl, 10 mM MgCl2, 0.01% BSA, 5 mM ATP, 1 mM DTT and 15 mM tetra(LRRASLG) peptide, and 40 ng Aurora B proteins) at 30 °C for 180 min. Following incubation, 50 μL Kinase-Glo Plus Reagent (Promega, Madison, WI, USA) was added, and the mixture was incubated at 25 °C for 20 min. A 70 μL aliquot of each reaction solution was transferred to a 96-well black microliter plate, and luminescence was measured on a Wallac Vector 1420 multilabel counter.

5.2.3 HCT-116 cell lines and MTS cell viability assay

HCT-116 cell viability was examined by MTS assay (Promega,Madison, WI). 2,000 HCT-116 cells in 100 μL of McCoy's 5a medium were seeded in each well of a 96-well plate. After the test compound was incubated in cells for 96 h, the cells were then incubated with 20 μL of a MTS/PMS mixture (MTS/PMS: 20/1) for 2 h at 37 °C in a humidified incubator with 5% CO_2 to allow viable cells to convert the tetrazolium salt (MTS) into formazan. The amount/concentration of formazan was determined by measuring the absorbance at 490 nm using a Perkin Elmer Wallac 1420 VICTOR2 microplate reader.

The MOLM-13 leukemia cell line was obtained from the Deutsche Sammlung von Microorganismen und Zellkulturen GmbH (DSMZ, Braunschweig, Germany). The Detroit-551, H1975, COLO205, and MV4-11 cell lines were also purchased from the American Type Culture Collection (ATCC, Manassas, VA, USA) and cultured

according to instructions of ATCC. To determine cell viability, cell assay for MOLM-13 and MV4-11 was performed by seeding 10,000 cells per well in a 96-well culture plate. The H1975 proliferation assays were performed by seeding 3,000 cells per well in a 96-well culture plate. Detroit-551 and COLO205 cells were seeded in culture plate at density of 2,500 and 4,000 cells per well. After 16 h, cells were then treated with vehicle or various concentrations of test compound in medium for 72 h. The viable cells were measured using the MTS method (Promega, Madison, WI, USA) according to the manufacturer's recommended protocol. Results were determined by measuring the absorbance at 490 nm using a plate reader (Victor2; PerkinElmer, Shelton, CT, USA). The CC_{50} value was defined as the amount of compound that caused a 50% reduction in cell viability in comparison with DMSO-treated (vehicle) control and was calculated using GraphPad Prism version 4 software (San Diego, USA).

5.2.3 In In vitro rat microsomal stability assay

The incubation mixture, in 74 mmol potassium phosphate buffer (pH 7.4), contained: microsomal proteins, 0.5 mg/mL; NADPH, 3 mmol; MgCl2, 3 mmol; test compound, 1 μM.. Incubation was carried out, in triplicate, aerobically at 37 °C with constant shaking on a temperature-controlled heating block. Reaction was started by the addition of NADPH after pre-incubating the reaction mixture (without NADPH) for 10 min at 37 °C. Control incubation without NADPH was performed as described above. At 0, 5,

10, 20 and 30 min after the start of reaction, an aliquot of the incubation mixture was taken from each incubation and mixed with ice-cold acetonitrile to terminate the reaction. Before analysis, the sample was precipitated by centrifugation at room temperature. The remaining supernatant was analyzed for the concentration of each compound to determine the metabolic rate [25].

5.2.4 In vivo pharmacokinetics studies in rats

The test compound was prepared by dissolving appropriate amount of compound in a solution formulation of DMA/PEG400 (20/80, v/v). Male Sprague-Dawley rats, weighing 250–400 g each (8–12 weeks old), were obtained from BioLASCO (Taiwan Co., Ltd, Ilan, Taiwan). A single 5.0 mg/kg and 20 mg/kg dose of compound was separately administered to groups of 3 rats each intravenously (IV) and oral route (PO), respectively. The dosing volume of solution was adjusted according to the rat body weight. At 0 (prior to dosing), 2, 5, 15, and 30 min and at 1, 2, 4, 6, 8, and 24 h after dosing, a blood sample was collected from each rat via the jugular-vein cannula and stored in 0–4 °C for further analysis. Plasma was obtained from the blood by centrifugation (14000 g for 15 min at 4°C in a Beckman model AllegraTM 6R centrifuge) and stored in a freezer (–20 °C). All samples were analyzed for the parent compound by LC-MS/MS instrument. Data were acquired by selected reaction ion monitoring. Plasma concentration data were analyzed with standard non-

compartmental method with software program (WinNonLin, version 1.1, Pharsight Corporation, CA). The studies were approved by Institutional Animal Care and Use Committee of National Health Research Institutes (Taiwan)[18].

Acknowledgments

Support from the National Health Research Institute and Ministry of Science and Technology, Taiwan (MOST 108-2314-B-400-005, MOST 108-2113-M-400-007, MOST 107-2113-M-400-001, MOST 106-2113-M-400-001, and MOST 105-2325-B-400-010 for H.P.H.) is acknowledged. This work is also financially supported by the Center of Applied Nanomedicine, National Cheng Kung University from The Featured Areas Research Center Program within the framework of the Higher Education Sprout Project by the Ministry of Education (MOE) in Taiwan. S.-Y.L. is supported by a postdoctoral fellowship from Ministry of Science and Technology, Taiwan (MOST 108-2811-M-400-501).

References

[1] F. Bray, J. Ferlay, I. Soerjomataram, R.L. Siegel, L.A. Torre, A. Jemal, Global cancer statistics 2018: GLOBOCAN estimates of incidence and mortality worldwide for 36 cancers in 185 countries, CA Cancer J. Clin., 68 (2018) 394-424.

[2] B. Kumar, S. Singh, I. Skvortsova, V. Kumar, Promising Targets in Anti-cancer Drug Development: Recent Updates, Curr. Med. Chem., 24 (2017) 4729-4752.

[3] R. Kannaiyan, D. Mahadevan, A comprehensive review of protein kinase inhibitors for cancer therapy, Expert Rev. Anticancer Ther., 18 (2018) 1249-1270.

[4] M.E.M. Noble, J.A. Endicott, L.N. Johnson, Protein kinase inhibitors: Insights into drug design from structure, Science, 303 (2004) 1800-1805.

[5] K.S. Bhullar, N.O. Lagaron, E.M. McGowan, I. Parmar, A. Jha, B.P. Hubbard, H.P.V. Rupasinghe, Kinase-targeted cancer therapies: progress, challenges and future directions, Mo.l Cancer, 17 (2018) 48.

[6] L. Zhang, R.J. Daly, Targeting the human kinome for cancer therapy: current perspectives, Crit. Rev. Oncog., 17 (2012) 233-246.

[7] P. Wu, T.E. Nielsen, M.H. Clausen, FDA-approved small-molecule kinase inhibitors, Trends Pharmacol. Sci., 36 (2015) 422-439.

[8] N. Berndt, R.M. Karim, E. Schonbrunn, Advances of small molecule targeting of kinases, Curr. Opin .Chem. Biol., 39 (2017) 126-132.

[9] J.M. Goldman, J.V. Melo, Chronic myeloid leukemia--advances in biology and new approaches to treatment, N. Engl. J. Med., 349 (2003) 1451-1464.

[10] M. Deininger, E. Buchdunger, B.J. Druker, The development of imatinib as a therapeutic agent for chronic myeloid leukemia, Blood, 105 (2005) 2640-2653.

[11] P. Wu, T.E. Nielsen, M.H. Clausen, Small-molecule kinase inhibitors: an analysis of FDA-approved drugs, Drug Discov. Today, 21 (2016) 5-10.

[12] E. Willems, M. Dedobbeleer, M. Digregorio, A. Lombard, P.N. Lumapat, B. Rogister, The functional diversity of Aurora kinases: a comprehensive review, Cell Div., 13 (2018) 7.

[13] A.C. Borisa, H.G. Bhatt, A comprehensive review on Aurora kinase: Small molecule inhibitors and clinical trial studies, Eur. J. Med. Chem., 140 (2017) 1-19.

[14] J.R. Pollard, M. Mortimore, Discovery and development of aurora kinase inhibitors as anticancer agents, J. Med. Chem., 52 (2009) 2629-2651.

[15] N. Keen, S. Taylor, Aurora-kinase Inhibitors as anticancer agents, Natute Rev. Cancer, 4 (2004) 927-936.

[16] G.S. Falchook, C.C. Bastida, R. Kurzrock, Aurora Kinase Inhibitors in Oncology Clinical Trials: Current State of the Progress, Semin Oncol., 42 (2015) 832-848.

[17] C.H. Cheung, S. Sarvagalla, J.Y. Lee, Y.C. Huang, M.S. Coumar, Aurora kinase inhibitor patents and agents in clinical testing: an update (2011–2013), Expert Opin. Ther. Pat., 24 (2014) 1021-1038.

[18] Y.C. Hsu, M.S. Coumar, W.C. Wang, H.Y. Shiao, Y.Y. Ke, W.H. Lin, C.C. Kuo, C.W. Chang, F.M. Kuo, P.Y. Chen, S.Y. Wang, A.S. Li, C.H. Chen, P.C. Kuo, C.P. Chen, M.H. Wu, C.L. Huang, K.J. Yen, Y.I. Chang, J.T. Hsu, C.T. Chen, T.K. Yeh, J.S. Song, C. Shih, H.P. Hsieh, Discovery of BPR1K871, a quinazoline based, multi-kinase inhibitor for the treatment of AML and solid tumors: Rational design,

synthesis, in vitro and in vivo evaluation, Oncotarget, 7 (2016) 86239-86256.

[19] H.Y. Shiao, M.S. Coumar, C.W. Chang, Y.Y. Ke, Y.H. Chi, C.Y. Chu, H.Y. Sun, C.H. Chen, W.H. Lin, K.S. Fung, P.C. Kuo, C.T. Huang, K.Y. Chang, C.T. Lu, J.T. Hsu, C.T. Chen, W.T. Jiaang, Y.S. Chao, H.P. Hsieh, Optimization of ligand and lipophilic efficiency to identify an in vivo active furano-pyrimidine Aurora kinase inhibitor, J. Med. Chem., 56 (2013) 5247-5260.

[20] M.S. Coumar, J.S. Leou, P. Shukla, J.S. Wu, A.K. Dixit, W.H. Lin, C.Y. Chang, T.W. Lien, U.K. Tan, C.H. Chen, J.T. Hsu, Y.S. Chao, S.Y. Wu, H.P. Hsieh, Structure-based drug design of novel Aurora kinase A inhibitors: structural basis for potency and specificity, J. Med. Chem., 52 (2009) 1050-1062.

[21] M.S. Coumar, C.Y. Chu, C.W. Lin, H.Y. Shiao, Y.L. Ho, R. Reddy, W.H. Lin, C.H. Chen, Y.H. Peng, J.S. Leou, T.W. Lien, C.T. Huang, M.Y. Fang, S.H. Wu, J.S. Wu, S.K. Chittimalla, J.S. Song, J.T.A. Hsu, S.Y. Wu, C.C. Liao, Y.S. Chao, H.P. Hsieh, Fast-forwarding hit to lead: aurora and epidermal growth factor receptor kinase inhibitor lead identification. J. Med. Chem. 53 (2010) 4980-4988.

[22] Y.Y. Ke, H.Y. Shiao, Y. Chang Hsu, C.Y. Chu, W.C. Wang, Y.C. Lee, W.H. Lin, C.H. Chen, J.T.A. Hsu, C.W. Chang, C.W. Lin, T.K. Yeh, Y.S. Chao, M.S. Coumar, H.P. Hsieh, 3D-QSAR-Assisted Drug Design: Identification of a Potent Quinazoline-Based Aurora Kinase Inhibitor, ChemMedChem, 8 (2013), 136-148.

[23] Y. Chang Hsu, Y.Y. Ke, H.Y. Shiao, C.C. Lee, W.H. Lin, C.H. Chen, K.J. Yen, J.T.A. Hsu, C. Chang, H.P. Hsieh, Facile identification of dual FLT3–Aurora A inhibitors: a computer-guided drug design approach, ChemMedChem, 9 (2014), 953-961.

[24] J. Chang, H. Ren, M. Zhao, Y. Chong, W. Zhao, Y. He, Y. Zhao, H. Zhang, C. Qi, Development of a series of novel 4-anlinoquinazoline derivatives possessing quinazoline skeleton: Design, synthesis, EGFR kinase inhibitory efficacy, and evaluation of anticancer activities in vitro, Eur. J. Med. Chem., 138 (2017) 669-688.

[25] H.T. Yao, Y.S. Wu, Y.W. Chang, H.P. Hsieh, W.C. Chen, S.J. Lan, C.T. Chen, Y.S. Chao, L. Chang, H.Y. Sun, T.K. Yeh, Biotransformation of 6-methoxy-3-(3',4',5'-trimethoxy-benzoyl)-1*H*-indole (BPR0L075), a Novel antimicrotubule agent, by mouse, rat, dog, and human liver microsomes, Drug Metab. Dispos., 35 (2007) 1042-1049.

[26] M.P. Pollastri, Overview on the Rule of Five, Curr Protoc Pharmacol, Chapter 9 (2010) Unit 9 12.

[27] M.Q. Zhang, Working with small molecules: rules-of-thumb of "drug likeness", Methods Mol. Biol., 803 (2012) 297-307.

[28] S. Tian, J. Wang, Y. Li, D. Li, L. Xu, T. Hou, The application of in silico drug-likeness predictions in pharmaceutical research, Adv. Drug Deliv. Rev., 86 (2015)

2-10.

[29] S. Mignani, J. Rodrigues, H. Tomas, R. Jalal, P.P. Singh, J.P. Majoral, R.A. Vishwakarma, Present drug-likeness filters in medicinal chemistry during the hit and lead optimization process: how far can they be simplified?, Drug Discov. Today, 23 (2018) 605-615.

[30] C.A. Lipinski, F. Lombardo, B.W. Dominy, P.J. Feeney, Experimental and computational approaches to estimate solubility and permeability in drug discovery and development setttings, Adv. Drug Deliv. Rev., 46 (1997) 3-26.

[31] B.J. Aungst, Optimizing Oral Bioavailability in Drug Discovery: An Overview of Design and Testing Strategies and Formulation Options, J. Pharm. Sci., 106 (2017) 921-929.

[32] C.A. Bergstrom, R. Holm, S.A. Jorgensen, S.B. Andersson, P. Artursson, S. Beato, A. Borde, K. Box, M. Brewster, J. Dressman, K.I. Feng, G. Halbert, E. Kostewicz, M. McAllister, U. Muenster, J. Thinnes, R. Taylor, A. Mullertz, Early pharmaceutical profiling to predict oral drug absorption: current status and unmet needs, Eur. J. Pharm. Sci., 57 (2014) 173-199.

[33] R. Rydzewski, Real World Drug Discovery. A Chemist's Guide to Biotech and Pharmaceutical Research, 1st ed., Elsevier Science, 2008.

[34] W.J. Egan, K.M. Merz, J.J. Baldwin, Prediction of drug absorption using

multivariate statistics. J. Med. Chem., 43 (2000), 3867-3877.

[35] W.J. Egan, G. Lauri, Prediction of intestinal permeability, Adv. Drug Del. Rev., 54 (2002), 273-289.

[36] https://www.discoverx.com/services/drug-discovery-development-services/kinase-profiling/kinomescan.

Declaration of interests

■ The authors declare that they have no known competing financial interests or personal relationships that could have appeared to influence the work reported in this paper.

☐The authors declare the following financial interests/personal relationships which may be considered as potential competing interests:

Graphical Abstract

Drug-Like Property Optimization: Discovery of Orally Bioavailable Quinazoline-Based Multi-Targeted Kinase Inhibitors

Shu-Yu Lin[a,#], Chun-Feng Chang[a,#], Mohane Selvaraj Coumar[d,#], Pei-Yi Chen[a], Fu-Ming Kuo[a], Chun-Hwa Chen[a], Mu-Chun Li[a], Wen-Hsing Lin[a], Po-Chu Kuo[a], Sing-Yi Wang[a], An-Siou Li [a], Chin-Yu Lin[a], Chen-Ming Yang[a], Teng-Kuang Yeh[a], Jen-Shin Song[a], John T.-A. Hsu[a], Hsing-Pang Hsieh [a,b,c*]

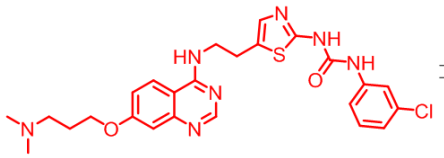

BPR1K871 (1)
PCP violation = 2
AURKA IC_{50} = 22 nM
AURKB IC_{50} = 13 nM
FLT3 IC_{50} = 19 nM
RLM (% remain @30 min) = 14.5%
Rat IV Clearance = 60.4 mL/min/Kg
No oral bioavailability (F = 0%)

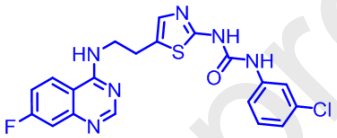

34
PCP violation = 0
AURKA IC_{50} = 9 nM
AURKB IC_{50} = 30.5 nM
FLT3 IC_{50} = 129 nM
RLM (% remain @ 30 min) = 77.8%
Rat IV Clearance = 13 mL/min/Kg
Oral bioavailability (F = 54%)

Physicochemical properties (PCPs) plot

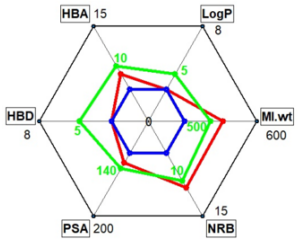

Optimal PCPs
BPR1K871's PCPs
Compound 34's PCPs

Highlights

- A series of quinazoline based analogues was designed and synthesized.
- We optimized our previous clinical candidate, BPR1K871, to improve the pharmacokinetics property and identify orally bioavailable lead.
- Compound **34** showed potent inhibitory activity against HCT-116 cells and exhibited good oral bioavailability of 54%.
- **34** also showed potency against several kinases especially the tyrosine kinases, including FLT3, DDR1, DDR2, TRKA, TRKB, and TRKC.